

Recent Developments in the Practical Philosophy of Ship Structural Design

By Egil Abrahamsen,¹ Member

Theories for description of the sea and calculation of the wave induced motions and loads on ships are briefly described and discussed. Results from calculations are compared to results from other calculations, model tests, and full-scale measurements. Reasonably good agreement is generally found and it is concluded that the results of calculations can be used for practical applications. Calculated largest expected values of some response variables are given.

Various aspects of the structural analysis and design of ships are investigated and discussed. This comprises, for example, experimental and analytical features pertaining to the torsional response of all-hatch ships, buckling phenomena for typical transverse girders, discontinuity problems in girders, rigidity and internal response of wash bulkheads, web frame design for oil tankers, evaluation of bilge tank torsional rigidity and its effect on the response of the double bottom. Moreover, problems concerning the longitudinal hull girder section modulus and slamming strength, have been considered in some detail.

A SHIP is a very complex structural system. The monocoque hull girder is divided into a number of separate compartments designed to maintain tightness and structural integrity under the loads imposed by the cargo in their compartments and by the sea loads and motions. The structure and its contents respond to the highly hostile environment as a highly elastic structural system with six degrees of freedom among a highly irregular wave system.

For hundreds of years, experience has been the governing factor in ship structural design. Until recent years, the growth in ship sizes has been slow, mainly because extrapolation based on empiricism must be slow.

In recent years the accumulation of new knowledge within subjects related to ship structural design has been extensive. Our theoretical knowledge, the experimental tools, and the mathematical and computational facilities to further improve on our knowledge have advanced tremendously.

Under these circumstances, it is reasonable to ask whether the classification societies which are responsible for the structural design of the greater part of our merchant ships, have realized the impact which our new knowledge and our new scientific tools should rightly have on an old empirical and later semi-empirical profession.

The author believes that all the bigger classification societies are eagerly concerned with all new developments. But the classification societies are simultaneously aware

that a structural design optimum in the sense that a complex system may be optimized, can within the framework of the traditional rules, at present only be achieved by parts.

Structural optimization can not be separated from the economical optimization of a ship over her lifetime. Structural optimization is further strongly dependent on the ratio between labor cost and cost of materials, and the optimum solution may be quite different in Japan and in the United States.

The basic aim of the classification societies should, however, be to approach the structural design problem firstly as a question of safety and see to it that in no case the total risk of structural failure is greater than society can accept. This risk should be measured against other risks to which man and property are subjected both on board and ashore.

Secondly, it should be borne in mind that cracks and small fractures necessitating frequent off hire for repairs, but which may be of such a nature that no risk for life or property is involved, may necessitate an increased strength and improved construction standards based upon economical considerations.

The classification societies should also aim at a balanced design such that the material is distributed in the structure according to the loads and such that the risk of failure is decreasing as the importance of a structural part becomes greater.

Judging from the damage cards collected by the Society

¹Managing Director, Det norske Veritas, Oslo, Norway.

over the last 15 years, one may conclude that the longitudinal strength standards developed and applied during that period seem to be reasonable, provided that the detail design and the workmanship is above a certain minimum standard, and that the hull material is selected according to the requirements. Practically none of the fractures have been of a type which might lead to total collapse of the hull structure. Even the rest of the failures which may be attributed to longitudinal stressing and which are of the nuisance type, have shown a markedly reduced frequency of occurrence. The ships in the length range from 140 meters to 180 meters show a somewhat higher fracture frequency than both larger and smaller ships.

On the other hand, the number of cracks and other types of damages to the internals in tankers have shown a somewhat increased frequency of occurrence in the larger ships. This tendency has necessitated a tighter control of the detail design, the design stresses and the loading of the internal structure of large ships, especially in cases where excessively long tanks are involved. Also the increased loading of the local structure at the ship ends due to the ship motions had to be taken more fully into account than previously. These measures have no doubt helped to create an improved balance between the longitudinal and the local strength of large ships.

It should be realized that both the loads on a ship and the structural strength of a ship or a part of the hull are statistical in nature. Even if the mass of statistical data available is relatively scanty, it seems natural today to base future ship structural developments on statistical models. Even if such models may be regarded as being in the embryonic stage, they may more clearly demonstrate where new information is most needed. No difficulty should be experienced in fitting prior knowledge into such models.

In the statistical approach to ship structural design it is essential to acquire knowledge of the statistical behavior of loads. It is equally important to realize that the structural strength of a ship and its many interacting components also follow certain statistical laws, even if the nominal strength is according to the same standard. The difference may be due to the freedom of selecting scantlings and structural systems within the framework of the standards, difference in detail design, in the properties of materials used, in welding and workmanship, and in control. During the life of the structure, overall and local corrosion may lead to reductions in strength which are strongly dependent on the maintenance work done.

Besides setting the nominal strength standards for new ships, the classification societies also maintain a system to control that none of their classed ships is wasted below a certain strength standard. If this is found to be the case, renewals are required. The longitudinal section modulus may, for example, not be reduced by more than 10 per cent before renewals are required.

Even if some ships may experience accelerated corrosion due to special cargoes or unsatisfactory maintenance such that the longitudinal section modulus may be reduced below the figure indicated, it is believed that the classification societies generally are in a position to keep the overall strength spectrum of their ships fairly narrow.

The strength spectrum for structural components will have a tendency to grow wider, the less important the structural part. For all parts the classification societies maintain both a nominal strength standard and a lower standard taking allowable corrosion, wear, and tear into account. By the statistical approach to the assessment of strength, distribution functions for strength of all ship structural components are needed in principle. In practice it will be sufficient to establish the distribution functions for a few characteristic components. Actually, these distribution functions will mainly have to be established by calculation supported by whatever model tests may be available. Already much material is in hand to form a basis for the estimation of strength distribution functions for ship structural components.

It is important to realize that the classification societies through their rules and their surveying practice have a very direct influence on both the position and the narrowness of these strength spectra.

Now "the strength" of a structural component or a system is no uniquely defined value, but is related to the definition of "failure." Failures may be divided in at least two categories, viz. "damage" and "collapse" as defined by I.S.S.C. Committee 10:

(a) *Damage* means that the structure has changed in a way which is detrimental to its future performance, even though there may be no immediate loss of function. Examples of damage include excessive permanent deformations resulting from local yielding or buckling, or the appearance of cracks due to fatigue or local brittleness. In such cases, the structure may still be able to sustain its design loads, but because of the possible adverse effects on performance or appearance, and hence on the confidence of operators and users, repairs should be effected as soon as convenient.

(b) *Collapse* means that the structure is damaged so badly that it can no longer fulfill its intended function. This loss of function may be gradual, as in the case of a progressing fatigue crack or spreading plasticity; or sudden, as when the failure occurs through plastic instability or through propagation of a brittle crack. In all instances, collapse is associated with a load history which will cause this loss of function.

Now in a true statistical approach, the limiting values of the strength or stiffness of a structure or a structural component, the "capability" of the structure should be measured against the "demand" on the structure provided by the environment to give a certain small risk of failure.

It is felt that time is not ripe for utilizing fully the statistical concept on this point, since too many uncertainties would have to be introduced. But we are working on the structural reliability problem also from this angle and believe that we eventually may establish the capability functions of characteristic ship structure components.

Within the scope of a short paper, it is difficult to treat the subject of ship structural design in more than its broader aspects. Therefore, the paper concentrates on a few characteristic features of the problems rather than to try to cover a great many different details.

PART I: Wave Induced Motions and Loads

A. Description of the Sea

The Short Term Distribution

By critically analyzing different wave spectra that have been proposed recently, we found that Pierson-Moskowitz spectrum is to be preferred. This spectrum [1]² may be defined by the following equation:

$$[a(\omega)]^2 = (\alpha g^2 / \omega^5) \exp[-\beta (\omega_o / \omega)^4] \quad (1)$$

$[a(\omega)]^2$ = wave spectrum

$$\alpha = 8.10 \cdot 10^{-3}$$

$$\beta = 0.74$$

$$\omega_o = g/U$$

U = wind speed reported by the weather ships.

Any consistent sets of units can be used.

Most wave statistics are given in terms of visually estimated wave periods T_v and wave heights H_v . We therefore write the Pierson-Moskowitz spectrum in the following nondimensional way:

$$\frac{[a(\omega)]^2}{H_{1/3}^2 \cdot \bar{T}} = (8\pi^2)^{-1} (\bar{T}\omega/2\pi)^{-5} \exp[-\pi^{-1}(\bar{T}\omega/2\pi)^{-4}] \quad (2)$$

This spectrum is shown in Fig. 1.

$H_{1/3}$ is the significant wave height defined as the mean of the upper third waves. \bar{T} is the average apparent wave period. $H_{1/3}$ and \bar{T} are related to the moments of the spectrum in the following way:

$$H_{1/3} = 4\sqrt{m_0} \quad (3)$$

$$\bar{T} = 2\pi\sqrt{m_0/m_2} \quad (4)$$

$$m_c = \int_0^\infty \omega^c [a(\omega)]^2 d\omega \quad (5)$$

m_c is the c 'th moment of the spectrum about the $[a(\omega)]^2$ axis.

The relationships between the theoretical quantities $H_{1/3}$ and \bar{T} on one hand and the visual quantities H_v and T_v on the other may be obtained by comparing values of $H_{1/3}$ and \bar{T} obtained from instrumental wave records with simultaneously obtained visually estimated values of T_v and H_v . Such data have been published by Cartwright [2]. Cartwright and Yamanouchi [3] also gave the least square linear relations between instrumental and visual values. However, we have found the following functions, shown in Figs. 3 and 4, to be more proper than linear functions:

$$H_v = 0.45 H_{1/3}^{1.39} \quad (6)$$

$$T_v = 0.052 \bar{T}^{2.42} \quad (7)$$

Many different expressions have been proposed by

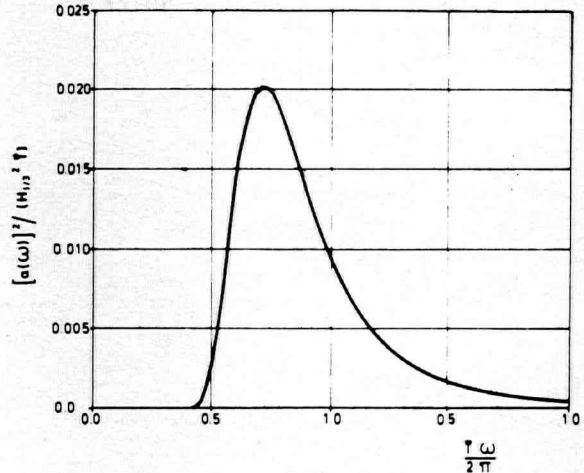


Fig. 1 The Pierson-Moskowitz wave spectrum

$$[a(\omega, \alpha)]^2 = [a(\omega)]^2 y(\alpha, \eta_s)$$

$$y(\alpha, \eta_s) = \frac{(\cos \alpha)^{\eta_s}}{K(\eta_s)}$$

$$K(\eta_s) = \int_{-\pi/2}^{\pi/2} (\cos \alpha)^{\eta_s} d\alpha$$

$$-\pi/2 \leq \alpha \leq \pi/2$$

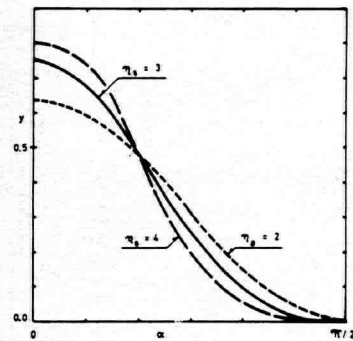


Fig. 2 The spectrum directionality function

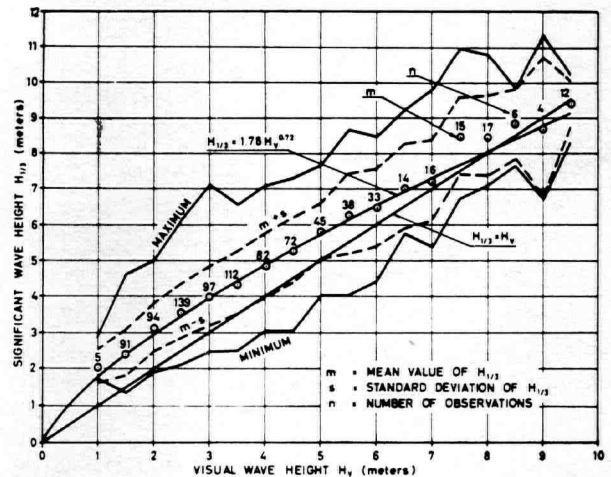


Fig. 3 Measured and visual wave height

²Numbers in brackets designate References at end of paper.

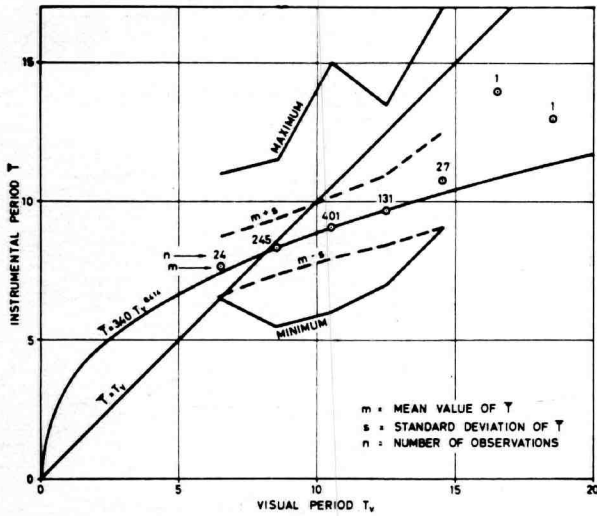


Fig. 4 Measured and visual wave period

various authors for description of the directionality of the waves. We have chosen the following function which fits reasonably well to the majority of the proposed functions:

$$[a(\omega, \alpha)]^2 = [a(\omega)]^2 (3/4) \cos^3 \alpha \quad (8)$$

for $-\pi/2 \leq \alpha \leq \pi/2$

α is the angle between the elementary wave and the wave system. The directionality function is shown in Fig. 2.

The Long Term Distribution

For computational purposes it is necessary to have a mathematical description of the long term statistical distributions of the parameters defining the short term states of the sea. Very little has been published on this subject, and therefore we found it necessary to develop a working method. We have found that the Weibull distribution function may be used to describe the long term distributions of H_V when T_V lies within small ranges.

$$P(H_V) = 1 - \exp \left\{ - \left[\frac{(H_V - H_0)}{(H_C - H_0)} \right]^\gamma \right\} \quad (9)$$

$P(H_V)$ is the probability that the visually estimated wave height does not exceed the value H_V . H_0 , H_C and γ are parameters of the distribution.

Fig. 5 shows Weibull distributions fitted to the data published by Roll [4] for the weather ships on the North Atlantic. For each range of T_V we get values of the parameters H_0 , H_C and γ . The long term description of the sea is thus reduced to a table of parameter values (see Table 1).

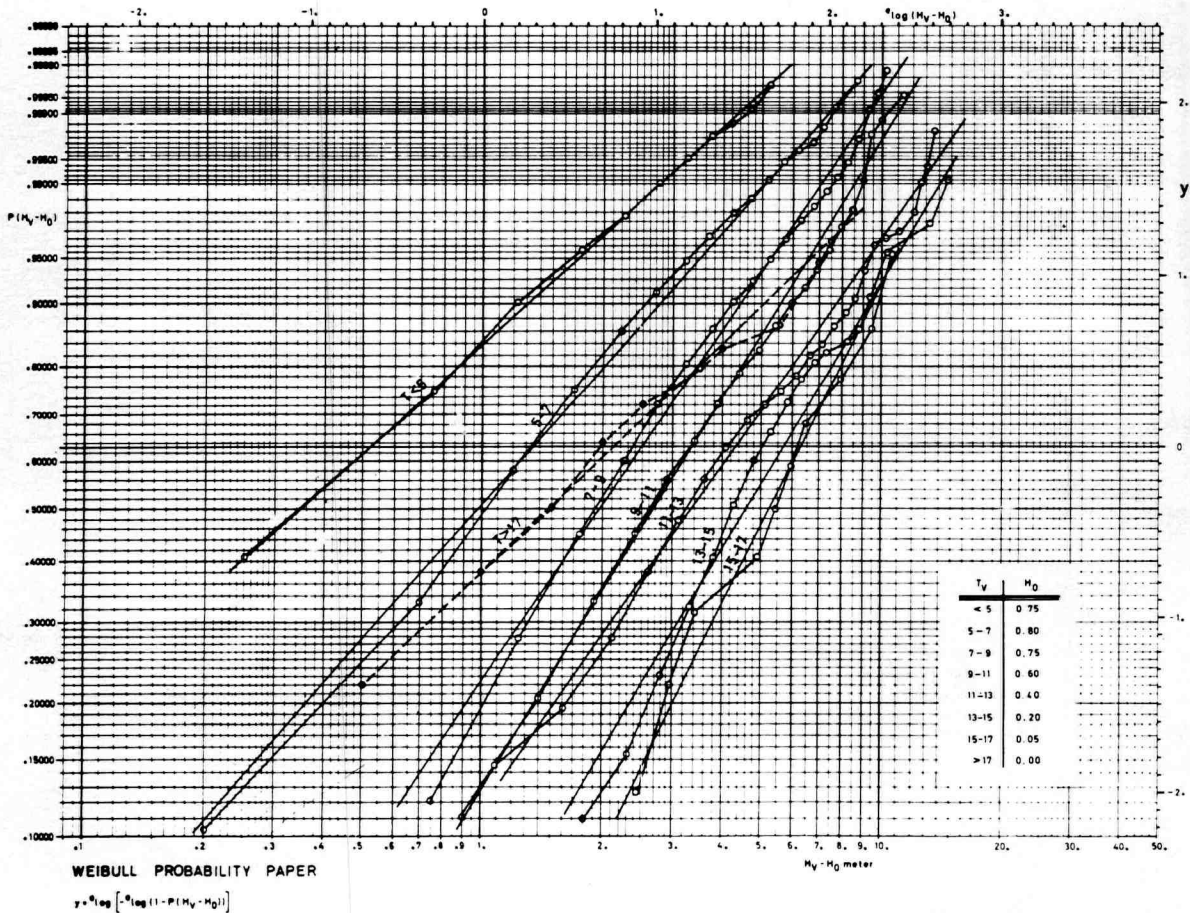


Fig. 5 Distribution of visually estimated wave heights in the North Atlantic. Summed up for the weather ships A-M. Data according to Roll [4]

Table 1 Distribution of Visually Estimated Wave Heights and Periods in the North Atlantic

$$P(H_v) = 1 - e^{-\left(\frac{H_v - H_0}{H_c - H_0}\right)^\gamma}$$

T_v	H_0	$H_c - H_0$	γ	$p(T_v)$
<5	0.80	1.35	1.14	0.3668
5-7	0.75	2.50	1.49	0.3068
7-9	0.60	3.30	1.60	0.1131
9-11	0.40	4.30	1.42	0.0243
11-13	0.20	5.70	1.71	0.0054
13-15	0.05	6.30	2.04	0.0011
15-17	0.00	2.10	0.96	0.0027
>17	0.75	0.52	0.91	0.1798

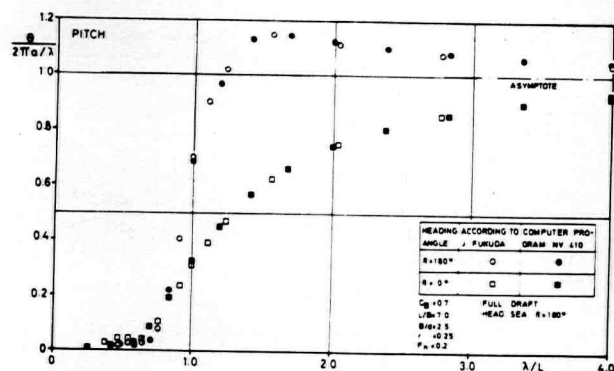


Fig. 6 Calculated transfer functions for Series 60

B. Ship Response

Regular Waves

The response in regular waves has been calculated by means of the strip theory of Korwin-Kroukowsky and Jacobs [5] and [6], and with coefficients for added mass and damping according to Grim [7]. We have compared the results from our calculations with the results from other calculations and with the results from model tests. Some examples of such comparisons are shown in Figs. 6-9.

Figs. 6 and 7 show comparisons with results according to Fukuda [8] from Watanabe's [9] strip theory with Tasai's [10] coefficients for added mass and damping. Generally the results are practically identical and none of the methods seems to be superior to the other.

Figs. 8 and 9 show comparisons with results from model tests according to Vossers, Swaan, and Rijken [11] and Swaan and Vossers [12]. Generally, the correlation between results from model tests and calculations are satisfactory. This holds not only for the influence of wave length, ship speed, and form of the sections as shown in Figs. 8 and 9, but also for variables such as block coefficient, length-beam ratio, beam-draft ratio, longitudinal radius of gyration and heading angle. Therefore, we consider the results from our computer program to be satisfactory for our practical purposes.

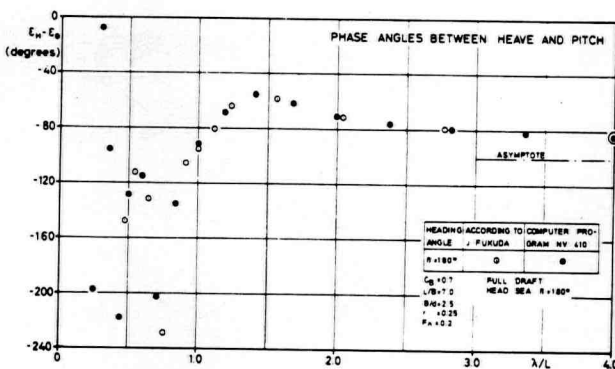


Fig. 7 Calculated phase angles for Series 60

Short Term Response

The short term response has been calculated from wave spectra and transfer functions according to the linear superposition technique. The log-slope method proposed by Lewis [13] has been used in these calculations. This method gives simpler calculations than the conventional method, and it makes it easier to understand how the re-

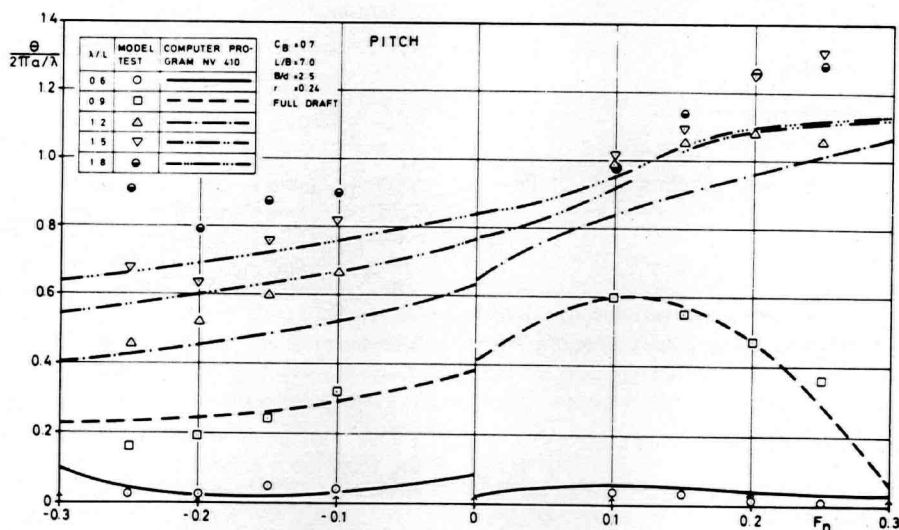


Fig. 8 Calculated transfer functions for Series 60 compared to model tests according to Vossers, Swaan, and Rijken [11]

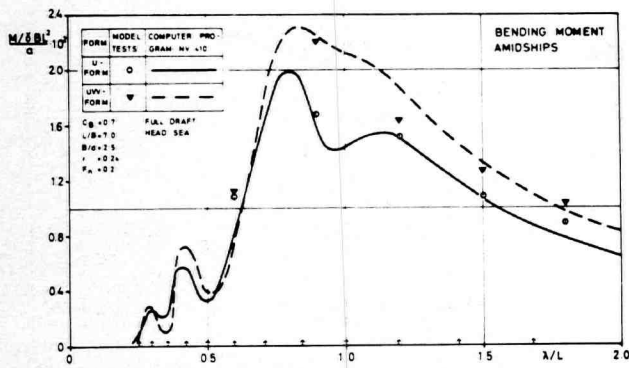


Fig. 9 Calculated transfer functions for Series 60 compared to model tests according to Vossers, Swaan, and Rijken [11]

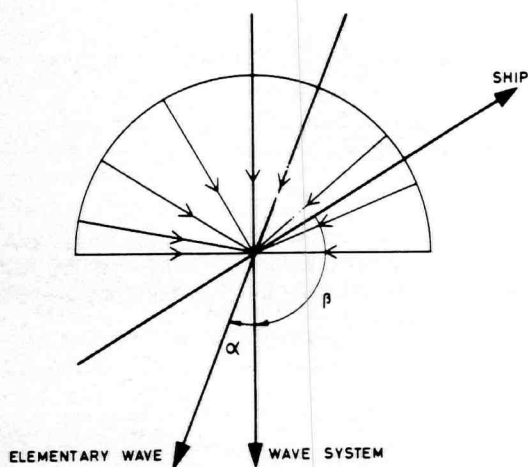


Fig. 10 Definition of angles

sponse is influenced by the ship length. The log-slope spectrum is related to the conventional spectrum in the following way:

$$\left[\frac{a(\ln \lambda)}{\lambda} \right]^2 = \frac{\omega^5}{2(2\pi g)^2} [a(\omega)]^2 \quad (10)$$

- $\lambda = 2\pi g / \omega^2$ is the wave length
- g = gravitational acceleration
- \ln stands for the natural logarithm

We write the long-slope transfer function in the following way:

$$\overline{TR}_x = \frac{x}{a/\lambda} \quad (11)$$

x is the single amplitude of a response variable in nondimensional form such as

- H/L for heave
- A/g for acceleration
- $M/\gamma B L^3$ for bending moment

- a = wave amplitude
- H = heave amplitude
- A = acceleration amplitude

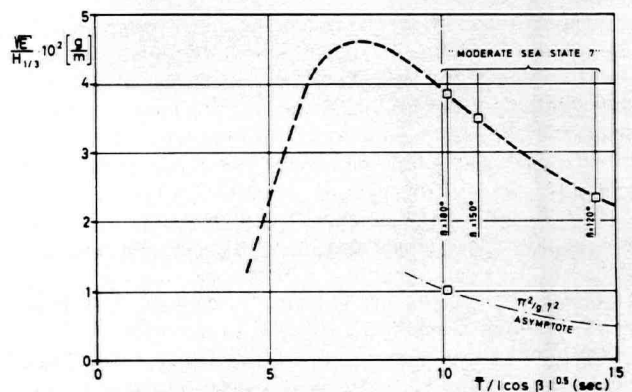
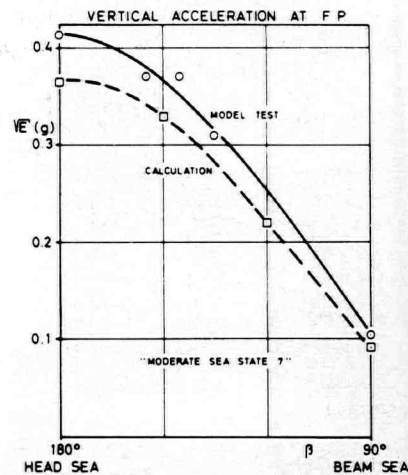


Fig. 11 Short term response in irregular waves. Mariner at light draft and 10 knots in long crested sea. Model tests according to Ochi [14]

- M = moment amplitude
- L = length of ship
- B = beam of ship
- γ = density of sea water

The variance of the response in a short-crested wave system is

$$s_x^2(\beta) = \int_{-\infty}^{\infty} \int_{-\pi/2}^{\pi/2} [\overline{TR}_x(\lambda, \alpha + \beta)]^2 [a(\ln \lambda, \alpha)/\lambda]^2 d\alpha d \ln \lambda \quad (12)$$

- α = angle between elementary wave and wave system
- β = angle between ship course and wave system
- α and β are defined in Fig. 10

$s_x^2(\beta)$ = variance of the variable x at heading angle β
 $\overline{TR}_x(\lambda, \alpha + \beta)$ = transfer function for the variable x at wave length λ and angle $(\alpha + \beta)$ between wave and ship course.

$[a(\ln \lambda, \alpha)/\lambda]^2$ = directional log-slope spectrum
 The parameter $E_x(\beta)$ of the Rayleigh distribution of the response variable x at heading angle β is finally obtained as:

$$E_x(\beta) = 2 s_x^2(\beta) \quad (13)$$

The short term Rayleigh distribution of x at a certain heading angle is:

$$P(x_1) = 1 - \exp(-\lambda_1^2 E_x) \quad (14)$$

$P(x)$ = probability that x does not exceed the value x .

Fig. 11 shows an example of a comparison between calculations and model tests in long crested irregular waves. It can be shown that in long crested waves the influence of heading angle is very simply obtained. The principle is shown in the figure. This procedure, however, is not strictly valid for short crested waves. As shown in Fig. 11, the correlation between the calculations and the model tests is satisfactory. This conclusion is generally valid for most response variables.

According to Ochi [14], the short term probability of slamming at a certain station along the ship can be obtained as:

$$P_s(\text{slam}) = \exp \left[-\frac{d^2}{E_{RM}} - \frac{\overline{RV}^2}{E_{RV}} \right] \quad (15)$$

and the short term distribution function of the slamming pressure is:

$$P_s(p > p_1/\text{slam}) = \exp \left[-\frac{(p_1 - p_*)}{2c E_{RV}} \right] \quad (16)$$

$$p = 2c \overline{RV}^2 \quad (17)$$

\overline{RV} = relative vertical velocity between ship and wave

p = slamming pressure

c = constant dependent upon the local form of the ship

p_* and \overline{RV}_* = threshold values above which slamming occurs

d = draft at the actual station

E_{RM} = twice the variance of relative vertical motion between ship and wave

E_{RV} = twice the variance of relative vertical velocity between ship and wave

$P_s(\text{slam})$ = short term probability of slamming

$P_s(p > p_1/\text{slam})$ = short term probability that the slamming pressure exceeds the value p_1 provided slamming occurs

A comparison between our calculations and Ochi's model tests regarding slamming is shown in Fig. 12. The correlation is reasonably good. So it seems possible to determine also the slamming characteristics of a ship by means of calculations.

A comparison between our calculations and full-scale measurements is shown in Fig. 13. The full-scale measurements are according to reference [15]. The calculated values refer to a Series 60 ship form with the same principal dimensions as the actual ships in normal service conditions and with the longitudinal radius of gyration $r = 0.24$. It has been assumed that the ship travels equally long time in all headings relative to the waves.

The Beaufort number has been related to visual wave height H_V and period T_V according to Roll [4] as shown

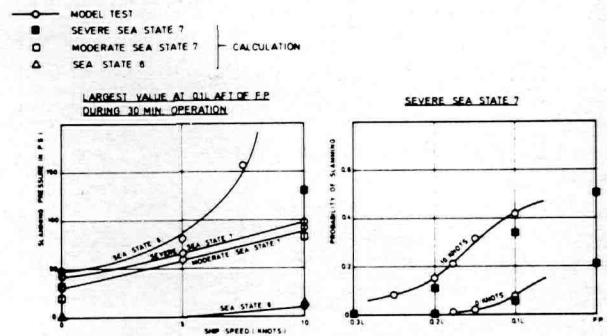


Fig. 12 Short term response in irregular waves. Mariner at light draft in long crested head sea. Model tests according to Ochi [14]

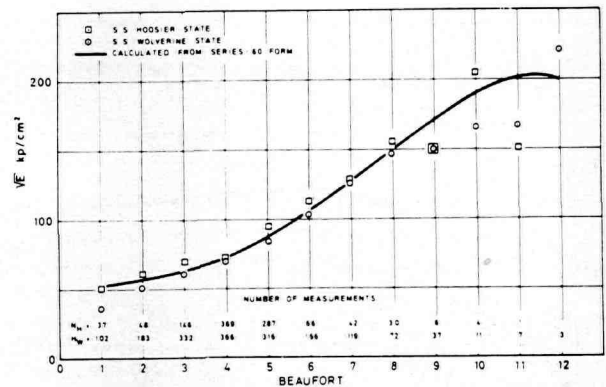


Fig. 13 Average \sqrt{E} values for peak-to-peak stresses amidships. Full-scale measurements according to Fritch, Bailey, and Wise [15]

in Table 2. The relationships between visual and theoretical wave height and period is according to equations (6) and (7) above.

As shown in Fig. 13, the correlation between the results of the full-scale measurements and the calculations are very satisfactory, and we are rather optimistic regarding the possibilities of predicting motions and loads on ships by means of calculations.

Long Term Response

The long term response of the ship when it travels in all kinds of sea states has been calculated by means of the

Table 2 Wave Height and Period as Function of Beaufort Force

Beaufort	According to Roll [4]		According to equations (6) and (7)	
	H_V	T_V	H_{calc}	T_{calc}
0	1.1	6.7	1.90	7.48
1	1.1	5.8	1.90	7.04
2	1.2	5.8	2.05	7.04
3	1.4	5.9	2.26	7.09
4	1.7	6.1	2.60	7.21
5	2.2	6.5	3.13	7.38
6	2.9	7.2	3.81	7.68
7	3.8	7.8	4.63	7.95
8	4.9	8.3	5.57	8.15
9	6.2	9.0	6.60	8.43
10	7.4	9.5	7.50	8.64
11	8.4	10.0	8.21	8.81
12	8.5	10.4	8.27	8.95

SHIP DATA	STATISTICAL STRAIN GAUGE SLAMMING INCLUDED			CALCULATED FROM FULL SCALE MEASUREMENTS OF \bar{E} SLAMMING NOT INCLUDED							
	SHIP No	1	2	3	4	5	6	7	8	9	10
TYPE OF VESSEL	GENERAL CARGO	GENERAL CARGO	GENERAL CARGO	GENERAL CARGO	GENERAL CARGO	ORE CARRIER/TANKER	ORE CARRIER/TANKER	TANKER	TANKER	TANKER	TANKER
DEADWEIGHT (tane)	10 750	8 450	6 550	4 600	8 600	14 100	21 700	34 200	48 500	58 500	
Lpp (m)	142.7	137.25	128.6	97.8	138.1	140.2	170.7	198.1	214.9	238.4	
BREADTH (m)	19.75	19.2	18.6	14.5	19.2	19.5	22.7	26.8	31.1	35.4	
DRAUGHT (m)	8.4	8.2	7.8	6.9	7.8	8.0	9.4	10.7	11.5	13.1	
BLOCK-COEFF C_B	0.674	0.657	0.628	0.68	0.66	0.77	0.79	0.77	0.80	0.80	
L/B	7.2	7.15	6.8	6.75	7.2	7.2	7.5	7.4	6.9	6.7	
B/d	2.35	2.3	2.4	2.1	2.45	2.2	2.4	2.5	2.7	2.7	
SERVICE SPEED (kn)	16.0	16.0	16.0	14.0	17.0	15.0	14.5	16.8	16.8	16.0	
PROUDE NUMBER	0.22	0.22	0.23	0.23	0.24	0.21	0.18	0.20	0.18	0.17	

* THE BLOCK COEFFICIENT IS OFTEN CONSIDERABLY REDUCED AT SERVICE DRAFT

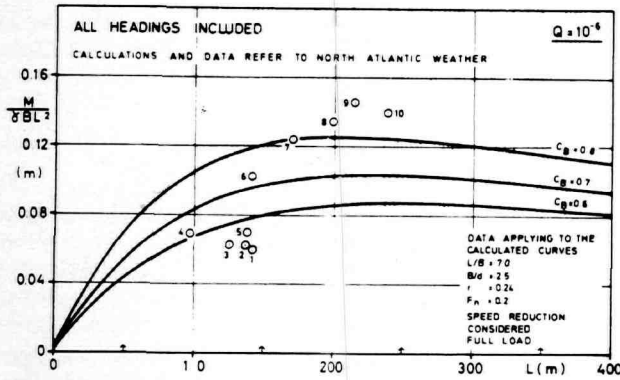


Fig. 14 Calculated largest expected bending moments on Series 60 at probability level $Q = 10^{-6}$ compared to full-scale data

method proposed by Nordenström [16]. An exhaustive description and discussion of this method will soon be published by Nordenström, but a short description will also be given below.

The procedure is as follows:

1 Describe the long term distribution of wave heights when the wave period lies within small intervals by means of the Weibull distribution function (see paragraph A).

2 Estimate

$$R = \sqrt{E/H_{1/3}} \quad (18)$$

as a function of T_V . We obtain R by means of calculations as described above.

3 Find the long term distribution $P(\sqrt{E})$ of \sqrt{E} from equations (6), (7), (9) and (18) in the following way:

$$P_i(\sqrt{E}) = 1 - \exp\left(-\left[\frac{0.45(\sqrt{E}/R_i)^{1.39} - H_{oi}}{H_{ci} - H_{oi}}\right]^{\gamma_i}\right) \quad (19)$$

Subscript i denotes that T_V lies within interval number i .

$$P(\sqrt{E}) = \sum_{i=1}^{NT} p_i P_i(\sqrt{E}) \quad (20)$$

p_i is the probability that T_V lies within interval number i .

4 Describe $P(\sqrt{E})$ by means of a Weibull distribution.

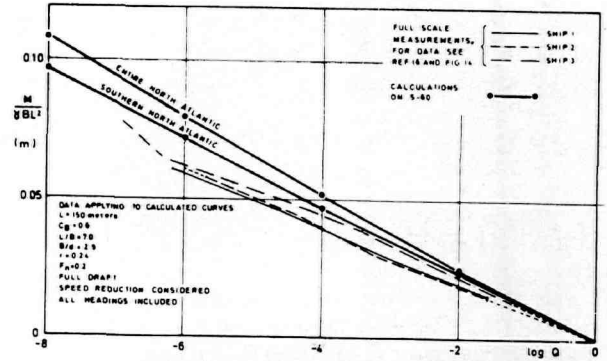


Fig. 15 Comparison regarding the type of calculated and measured long term distributions

$$P(\sqrt{E}) = 1 - \exp(-[\sqrt{E}/a]^m) \quad (21)$$

The parameters a and m are estimated from the calculated distribution (equation 20).

5 Estimate the long term distribution of the variable x from the following Weibull distribution.

$$P(x) = 1 - \exp\left(-\left[\frac{(x/a)^2}{b}\right]^k\right) \quad (22)$$

The parameters b and k are functions of m given in reference [16].

6 Estimate the long term distribution of x from equation (22) for different heading angles β and calculate the final long term distribution of x as

$$P(x) = \sum_{j=1}^{N\beta} p_j P_j(x) \quad (23)$$

where subscript j denotes that β lies within interval number j and p_j is the probability that the heading angle lies within interval number j .

The long term distribution of slamming pressures can not be obtained directly in the explicit form (equation 22). However, by introducing

$$\frac{1}{E_{slam}} = \frac{d^2}{E_{RM}} + \frac{\overline{RV}_*^2}{E_{RV}} \quad (24)$$

the following equation is obtained from equations (15) and (24)

$$P_s(\text{slam}) = \exp(-1/E_{slam}) \quad (25)$$

The parameters a and m in the long term distribution (equation 21) of $\sqrt{E_{slam}}$ can be obtained as described above and thus the long term probability of slamming is obtained from

$$P(\text{slam}) = 1 - \exp\left(-\left[\frac{(1/a)^2}{b}\right]^k\right) \quad (26)$$

Also in this case different heading angles can be considered according to equation (23).

The long term distribution of slamming pressures is obtained by repeating the previously mentioned procedure for different values of p_* [see equations (17) and (24)].

Some comparisons between results from full-scale meas-

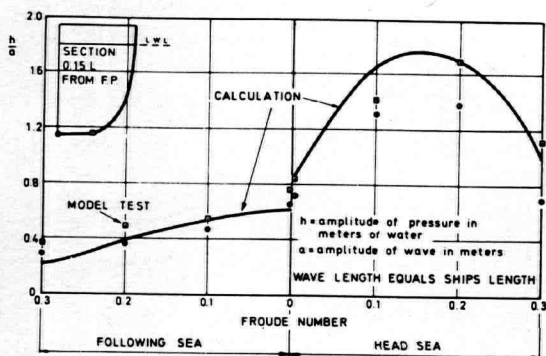


Fig. 16 Comparison between bottom pressures on a T-2 tanker calculated with computer program NV 403 and measured by Hoffman [24]

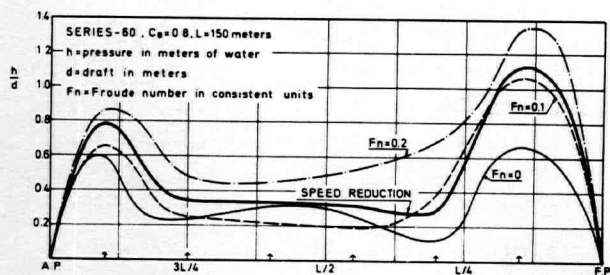


Fig. 17 Calculated largest expected bottom pressure on a T-2 tanker in head seas

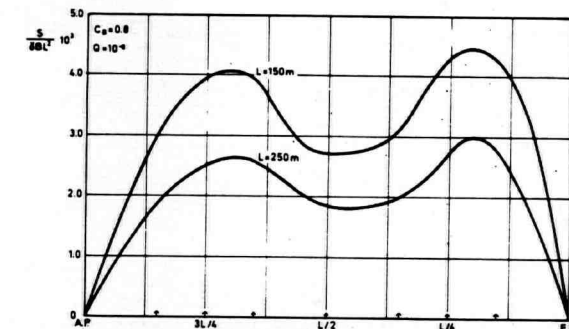
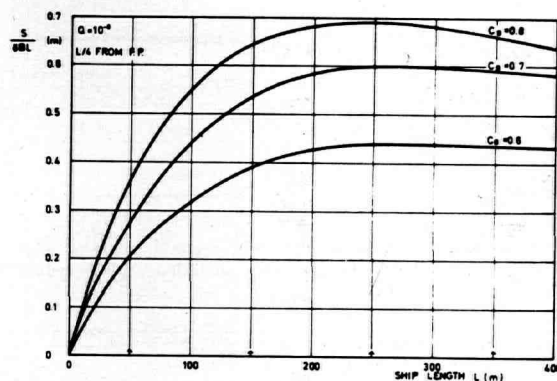


Fig. 19 Calculated largest expected vertical shearing force on Series 60 in head seas. Trapezoidal weight distribution with radius of gyration 0.24

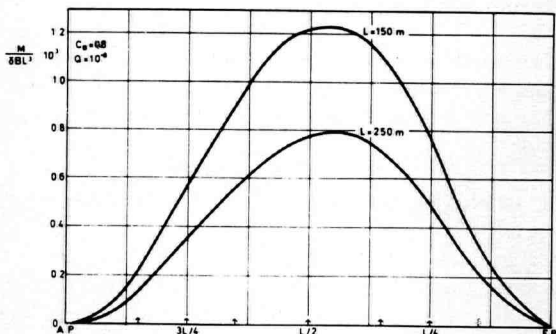
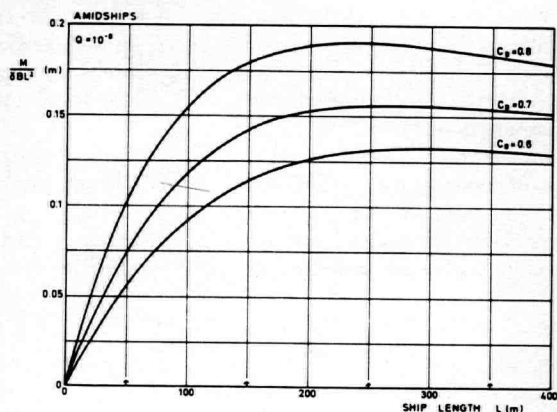


Fig. 18 Calculated largest expected vertical bending moment on Series 60 in head seas. Trapezoidal weight distribution with radius of gyration 0.24

urements and calculations are shown in Figs. 14 and 15. Because of lacking full-scale data, it is too early to come to any definite conclusions from this comparison. However, it seems as if the magnitude of the calculated values are rather favorable as compared to the full-scale data as shown in Fig. 14. Also the type of the long term distributions seems to be reasonable as shown in Fig. 15.

C. Some Results

No exhaustive description and discussions of the results from our calculations of long term distributions will be given here, but some examples of results hitherto obtained are shown in Figs. 17–25. It has here been assumed that the ships spend all their time on the North Atlantic and the weather is taken as the average for the weather ships A-M according to Roll [4].

It has also been assumed that the ships reduce their speed in heavy weather according to a criterion based on the probabilities of slamming and bow submergence. We have chosen a threshold function for these probabilities. This function goes from zero at full ship speed and to 0.5 at zero ship speed. This means that practically full speed is maintained when the probabilities are small, that the speed decreases when the probabilities increase and that the ship can not maintain forward speed at all when one of the probabilities exceed 0.5, that is, when the ship slams or submerges its bow every second wave encounter. The used criterion gives curves of speed versus weather which are very similar to the corresponding

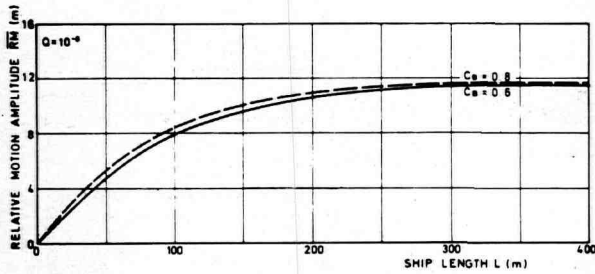


Fig. 20 Calculated largest expected vertical relative motion amidships on Series 60. All headings included. Speed reduction in heavy weather considered

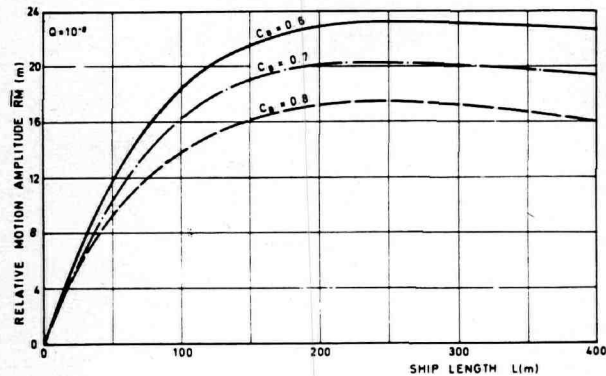


Fig. 21 Calculated largest expected vertical relative motion at 0.1 L from the forward perpendicular on Series 60. All headings included. Speed reduction in heavy weather considered

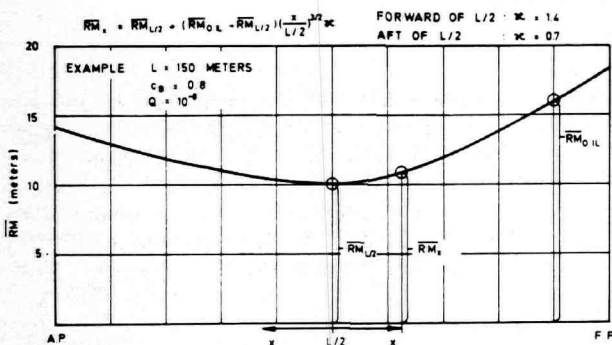


Fig. 22 Distribution of relative motion over the length of the ship

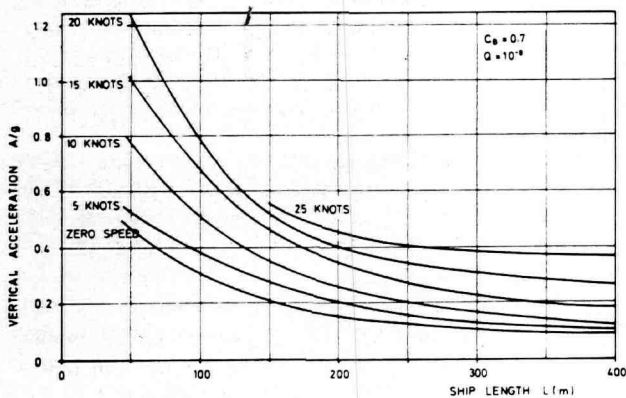


Fig. 23 Calculated largest expected vertical acceleration amidships on Series 60. All headings included. Speed reduction in heavy weather considered

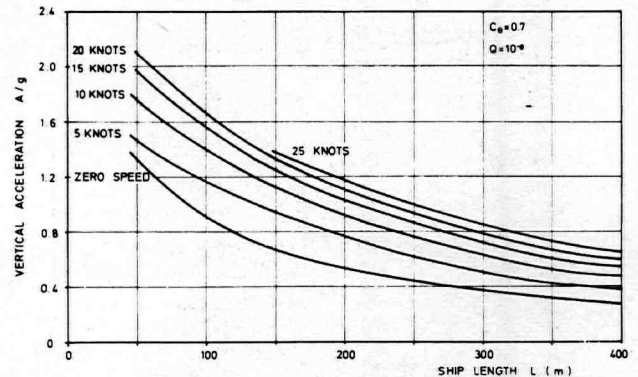


Fig. 24 Calculated largest expected vertical acceleration at forward perpendicular on Series 60. All headings included. Speed reduction in heavy weather considered

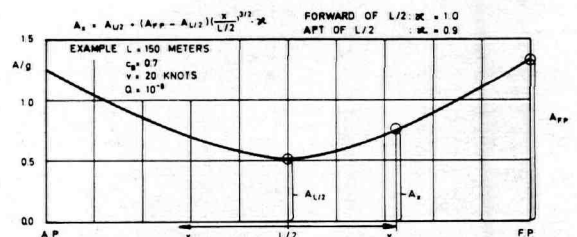


Fig. 25 Distribution of vertical acceleration over the length of ship

curves obtained from observations on ships. The speed reduction due to heavy weather has a small influence on bending moments and shearing forces, but it has a larger influence on bottom pressure and relative motion and a very large influence on accelerations. The results for the latter variables are therefore less reliable than those for the former.

We are now working on a rather extensive investigation of the influence of parameters such as length, beam, draft, speed, and fullness, and of factors such as shape of sections, weight distribution, and sea zone on the long term distributions of wave induced ship motions and loads.

PART II: Still Water Loads

General requirements to make ships easier to build and operate have led to certain problems in connection with the still water loading of ships. The still water loading for tankers may especially be aggravated by the requirements that:

- 1 The number of cargo tanks shall be as small as possible and the volume of each tank correspondingly large.
- 2 The possibilities of cargo segregation shall be reasonably wide.
- 3 The amount of clean ballast capacity shall be ample.
- 4 It should be possible to dock a ship with a fair amount of ballast.
- 5 Cargo tanks may be arranged for flume stabilization of the ship.

For bulk carriers, the condition that a certain number of the cargo holds, usually every second hold, may be empty when the ship is in the fully loaded condition, and

also the condition that one or more holds should be suitable for water ballast purposes, may influence the still water bending and shearing in an unfavorable way.

The small number of tanks in present day large tankers together with the requirement to clean ballast tanks reduces to a great extent the possibility to distribute the loading such that the still water bending moment and shear forces may be kept at a low level as could be done with the earlier type of tankers having from 30 to 45 different cargo tanks. With the large tanks, it may be quite possible to have the largest still water bending moment quite a distance from amidships and the biggest shear forces due to the still water loading may occur within the central part of the cargo tank range. Usually no great problems exist in connection with the evaluation of the still water bending moment and shear force distribution once the loading conditions have been defined.

It should be mentioned, however, that loading instruments intended to give the master information about the still water stressing of the ship, may be of little value if the instruments are not built to calculate both bending moments and shear forces at a number of critical sections. This also applies to bulk carriers with loads in alternate holds, in which case the still water bending moment and shear force distributions are quite different from what one would expect from homogeneously loaded ships.

To take care of these load distribution problems, classification societies today work out a large set of practical load distributions which may be allowed for each ship.

Mention should be made, however, of some necessary corrections to the traditional and somewhat simplified methods of still water bending and shearing calculations. The remarks will have bearing also on the wave bending and shearing calculations, but usually the resulting influence may in this case be so small that it may be disregarded.

With the great difference in load which may be experienced in neighboring cargo spaces, both in tankers and in bulk carriers, where one hold may be completely loaded and the neighboring hold may be completely empty, the concentration of loads caused by a transverse bulkhead should be evaluated carefully. When calculating the still water bending moment and shear forces from such load distributions, the direct integration of the difference between weight and buoyancy along the ship hull may give quite erroneous results. Before the integration is performed, one should in such cases always study how the loads on the bottom of the cargo compartments are distributed both to the ship sides and to the longitudinal and the transverse bulkheads. That part of the weight or buoyancy forces which are carried by for instance a transverse bulkhead, will be transferred as concentrated loads to the side shell from the longitudinal bulkheads. If the forces transferred to the bulkhead from each of the adjacent cargo compartments have opposite signs, the concentrated loads transferred to the ship sides may be more or less cancelled out. This is the case when we have a loaded hold on one side of a transverse bulkhead and an empty hold on the other side of the transverse bulkhead, as is usual in present-day bulk carriers. This

may effect a considerable reduction in the shear force as compared to the results from the traditional way of calculating the shear force distribution. Also, the longitudinal bending moment may be considerably influenced by this effect.

Mention should further be made of the considerable shear-lag effect which has been demonstrated by Schade [27] in connection with load distributions of the type to which modern bulk carriers are usually subjected.

Especially for larger ships, with small L/D ratios the still water bending moments and shear forces generally increase more rapidly than the wave bending moments with ship length. Generally, one will find that for very large ships, the "Square-cube law" will be fully operative for the still water loading, but not for the wave loading.

PART III: Structural Problems

A. Torsion of All-Hatch Ships

During the last two years we have studied the problem of torsion of hulls having extremely wide hatch openings. The principal purposes of this particular study comprised:

1 By virtue of a structural steel model to investigate the effects of various structural configurations.

2 To develop an analytical method by which the structural analysis of such ships could be executed with reasonable precision.

Fig. 26 gives an impression of the basic experimental model and the loading arrangement. The testing program was planned so that the basic model could be modified in proper succession, and thus provide structural configurations which aimed at the study of the following influences: (1) Variable hatch widths, (2) variable hatch corner radii, (3) transverse torsion boxes, (4) end conditions as influenced by a gradual increase in an additional hatch opening in one end of the ship, and (5) variable width of transverse deck girders or strips.

Some of these items have also been studied by other investigators, for example [18], consequently our efforts were primarily intended to extend and widen the knowledge in this field.

The linear dimensions of the steel model reflects a 1:45 scale ship. Certain difficulties involved in the fabricating process, however, limited the plate thickness to 3 mm.

Fig. 27 shows typical twist response diagrams for three

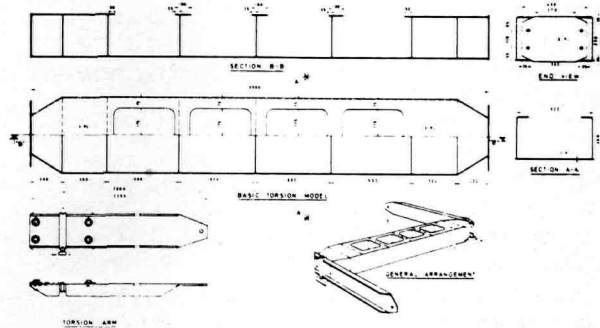


Fig. 26 Experimental model and loading arrangement

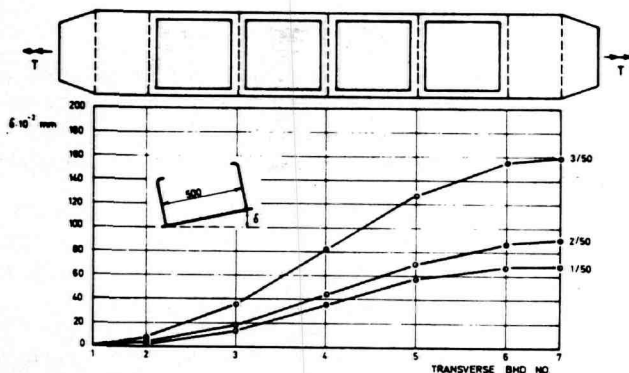


Fig. 27 Torsional rotation for three cut-out configurations due to a torque $T = 100$ kpm

different hatch widths, namely 70, 80, and 90 percent of the total ship breadth.

Furthermore, Fig. 28 contains information regarding stress distribution in the longitudinal deck girder adjacent to the end ship. This particular model had a hatch width of 90 percent, and hatch corner radii equal to 25 mm. Stress concentrations are seen to be very significant. Our experimental program involved three different hatch corner radii, $R = 50, 25,$ and 12.5 mm, for every width of the hatch opening. Furthermore, one version comprised two types of elliptical corners.

Our analytical efforts were based upon the fundamental differential equation for torsion of thin-walled beams subjected to transverse torsional loads. (It is to be noted that longitudinal tractions may contribute to the load term.) Therefore,

$$d^4 \theta / dz^4 - (k/l)^2 d^2 \theta / dz^2 = f(z) \quad (27)$$

where:

- θ = rotation of cross section about the shear center
- z = coordinate along the hull
- k = $[C^2 EJ_w]^{1/2}$
- C = torsional rigidity in pure torsion
- E = Young's modulus
- J_w = sectorial moment of inertia with respect to the shear center (the quantity EJ_w may be denoted sectorial rigidity, associated with normal stresses in the cross section)
- l = reference length
- $f(z)$ = loading term

It is important to notice that the quantity, C , comprises the equivalent effect of possible multiple deck transverses, as well as the properties of closed boxes in the cross section.

The general solution to equation (27) may be shown to be,

$$\theta(z) = C_1 + C_2 z + C_3 \sin h(kz/l) - C_4 \cos h(kz/l) + \theta_p(z) \quad (28)$$

The constants C_1, \dots, C_4 must be determined from appropriate boundary conditions. The quantity, $\theta_p(z)$, constitutes a particular integral of $f(z)$.

When the quantity, k , is equal to zero (or nearly so), the solution to equation (27) may be written as follows;

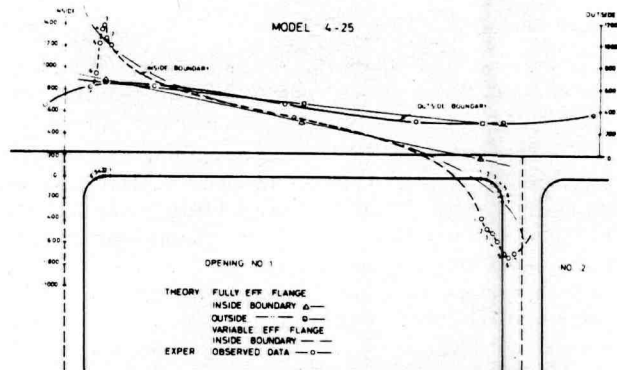


Fig. 28 Normal stresses along the boundaries due to a torque $T = 200$ kpm. Stresses in kp/cm^2

$$\theta(z) = A_1 + A_2 z + A_3 z^2 + A_4 z^3 + \theta_p(z) \quad (29)$$

where A_1, \dots, A_4 , constitute coefficients which are to be found by means of appropriate boundary conditions, and $\theta_p(z)$ represents a particular solution consistent with the modified differential equation. Equation (29) comprises an alternate solution which—under certain conditions—may prove to be satisfactory.

The boundary conditions are usually of the subsequent types, (a) clamped (kinematical relations), (b) hinged (mixed relations), (c) free (statical relations), and (d) elastic.

There are two conditions at each end. Item (d) comprises the elastic "foundation" provided by the end ships.

We applied the basic theory as indicated herein to one of the model configurations, and the results are shown in Fig. 28. The nominal stress distribution is observed to match the experimental observations well; while the stress concentrations in the hatch corners are not taken care of by this theory. Proper concentration factors should then supplement this procedure, and further reference is made to reference [19].

It is also mentioned that deformation estimates were found quite satisfactory.

Regarding the magnitude of the wave introduced torque amidships for actual ships, there exist considerable uncertainties. Measurements on actual ships have shown that the ratio of the maximum wave bending moment to maximum wave torque, is of the order of 10–20. We are presently assuming that a reasonable maximum wave torque at a probability level $Q = 10^{-8}$, may be given by:

$$T_m = C_T L B^3 \quad (30)$$

where:

- L = length between perpendiculars
- B = breadth moulded

C_T is a factor given as a function of the waterplane coefficient CW_L in Table 3, and that the variation of the wave torque along the ship may be approximated by,

$$T(z) = 0.62 T_m [\sin U - \sinh U - 1.02 (\cos U - \cosh U)] \quad (31)$$

where $U = 4.73 z/L$ and the variable, z , originates amidships.

CT	2.1	3.0	3.2	5.4
CWL	0.6	0.7	0.8	0.9

The previous torque relation depicts a variation along the hull analogous to the fundamental mode of a fixed-fixed beam. The coefficient, C_T , is herein intended to apply to open ships, that is, where the shear center is positioned well below the bottom.

It is normally experienced that the nominal torsion stresses in "open" ships are rather small, as compared to regular bending stresses. Nevertheless, it is good practice to consider local deck stresses with care, and be as generous as possible with regard to hatch corner radii.

Moreover, when it comes to the analysis and design of the hull, it is advisable to consider the possibility of skew loading as well as wave effects.

A much more comprehensive presentation of our findings with regard to torsion of "open" ships, may be found in a recent paper by Røfren [19]. Further information on this particular topic has also recently been discussed by Wilde [20].

Our experimental program resulted in the following conclusions:

1 The rotational flexibility of the hull is strongly increased when the hatch width is more than 80 percent of the total breadth.

2 A significant reduction in transverse deck girder rigidity results in a minor increase in rotational flexibility, and much pronounced reduction is maximum hatch corner stresses.

3 Transverse torsion boxes constitute very efficient means for reducing torsional flexibility and stresses.

4 An additional 50 percent hatch opening (hatch breadth ship breadth) in one end ship does not alter stresses noticeably. However, when this new hatch opening constitutes about 60 percent of the breadth, the maximum stresses in the original adjacent hold have decreased markedly, and much higher stresses are observed in the new hatch corners.

5 Stress concentrations in hatch corners are substantial. Elliptic corner configurations of usual proportions do not seem to offer any particular advantages.

6 Simple transverse bulkheads have no essential influence on the torsional rigidity, but serve primarily to maintain cross-sectional form.

7 General torsion theory as sketched herein, and more completely in [19], appear to give satisfactory results with respect to deformations and nominal stresses. In conjunction with overall torsional effects, it is emphasized that the wave environment also imposes certain local influences on the behavior of deck strips and other components, which in turn must be judiciously combined with the overall response of the hull.

B. Shear Flow Calculation for a Hull Section

The hull girder of an tanker of common design has essentially four webs connecting the bottom and deck flanges. For ships above a certain size, the shear-forces on the hull girder must be taken into account when deciding the thicknesses and the stability characteristics of

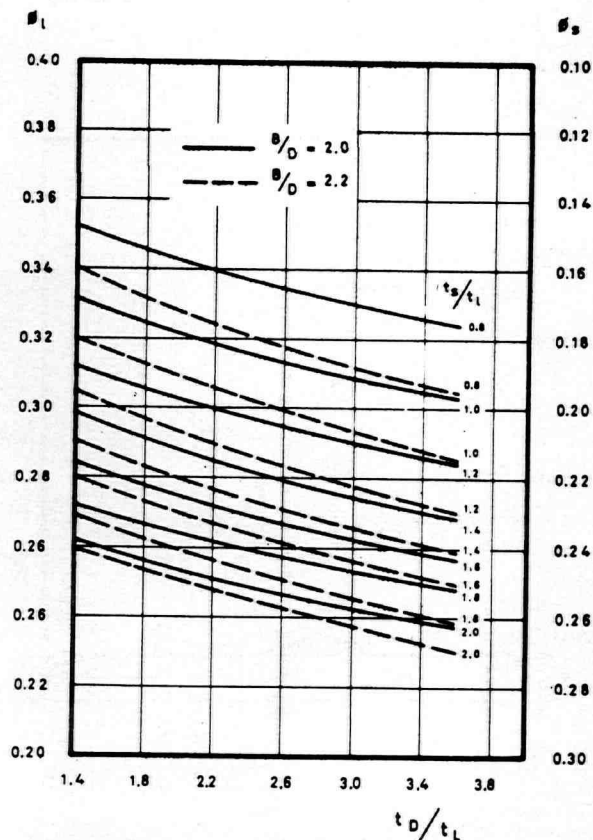


Fig. 29 Diagram for shear flow coefficients ϕ_L and ϕ_S

the plating in ship side and in longitudinal bulkheads. To this end it also becomes of importance to know how the longitudinal shear-force is distributed between ship sides and longitudinal bulkheads.

Today it is possible, of course, to calculate with great accuracy the entire stress distribution in a hull girder. For rule purposes, more approximate but reasonably accurate methods have to be applied.

In the case of a symmetrical structure such as a ship, it is obvious that when no centerline bulkhead is present, the shear stress will be zero at the centerline. In the absence of any torsional moment, the twist in each shell of the structure must be zero. Basing on these assumptions, the shear flow distribution around the shell may be calculated.

The maximum shear stress at a neutral axis in the longitudinal bulkhead and ship side plating, respectively, may be given thus:

$$\tau_l = \frac{F \cdot \Phi_l}{D \cdot t_l} \quad (32)$$

$$\tau_s = \frac{F \cdot \Phi_s}{D \cdot t_s} \quad (33)$$

where:

τ_l = the shear stress in the longitudinal bulkhead at the neutral axis

τ_s = shear stress in the side plating at the neutral axis

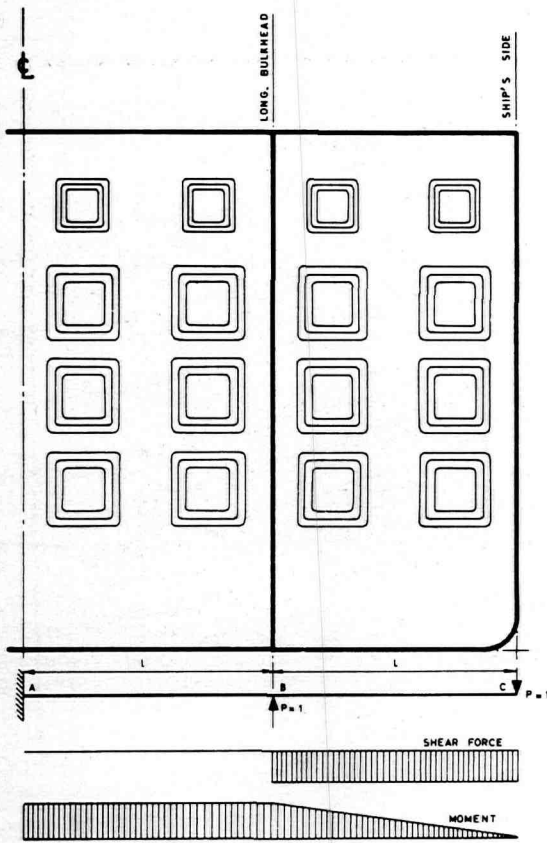


Fig. 30 Cut-out arrangement and loading scheme

- t_l = thickness of longitudinal bulkhead at neutral axis
- t_s = thickness of side plating at neutral axis
- D = depth of the ship
- F = total shear force on the cross section considered

Φ_l and Φ_s are factors which may be obtained from Fig. 29 on the basis of the parameters shown.

Notice that t_L , t_S , and t_D in Fig. 29 constitute equivalent or "smoothened" quantities, that is, the cross-sectional areas of plating, longitudinal stiffeners, and girders have been replaced by an equivalent thickness extending over a corresponding distance of the contour.

It is easily seen that with the common practice of using much greater thicknesses in the side shell than in the longitudinal bulkheads, the shear stresses in the longitudinal bulkheads may become much larger than in the side shell. The longitudinal bulkheads have perhaps mainly been regarded as a local structure whose main function has been to form tank boundaries. To use the steel material in a rational way, it seems natural to consider the longitudinal bulkheads in tankers as the most important web in the hull structure connecting the deck and bottom flanges. At least for the biggest ship types it will be natural to increase the thickness of the longitudinal bulkheads considerably more than the side plating. This would be welcome also from the point of view of local stress perturbations from transverse bulkheads and transverse webs landing on the longitudinal bulkheads.

These stress perturbations will usually be less in the ship side. On the other hand, it is necessary to secure a reasonable lateral strength of the side shell to prevent small dents from quays and towboats from causing disasters. This is, however, a question which is not solved by the right choice of side shell thickness, it is more a matter of adequate stiffening.

Furthermore, it is expected that applications of the finite element technique will shed further light on analytical problems associated with structural "beam-type" idealizations.

C. In-Plane Stiffness of Bulkheads and Some Problems Concerning the Bottom Grillage

The ships sides, as well as the longitudinal and transverse bulkheads, provide the principal supports for the bottom and deck structures. In view of the overall geometry of the transverse bulkheads, it may be deduced that their in-plane distortion is mainly due to shear. With large cutouts, the in-plane stiffness of a wash bulkhead may be considerably reduced due to the bending and shearing flexibility of the material between the cutouts. Especially in larger ships, large cutouts in wash bulkheads may have a detrimental effect on the boundary support which such a bulkhead should provide for the bottom girder system, and wash bulkheads should be designed with the utmost care. In particular, it is important to observe that an increase in the number of longitudinal girders of the bottom grillage, tends to enhance markedly the forces which the bulkheads must transport transversely.

In order to evaluate the in-plane stiffness of bulkheads with and without cutouts, we have carried out a series of theoretical investigations, applying the finite element technique. The results have been checked by measurements on a bulkhead model made in acryl and also by full-scale measurements.

The four different cases investigated theoretically had cutouts corresponding to 0, 10, 20, and 30 percent of the bulkhead area (see Fig. 30). The edges of the cutouts were not stiffened beyond the stiffening which existed in the bulkhead with no cutout.

The intention of the investigation was to obtain correction figures for the effective shear and bending rigidity, which in turn could be applied directly to the formulas obtained by elementary beam theory. The basic load system applied is shown in Fig. 30. Elementary theory gives the deflections at B and C according to the following expressions:

$$\delta_B = \frac{Pl^3}{2EI_{eff}} \quad (34)$$

$$\delta_C = \frac{11 Pl^3}{6 EI_{eff}} + \frac{Pl}{GA_{eff}} \quad (35)$$

or solved for I_{eff} and A_{eff} :

$$I_{eff} = \frac{Pl^3}{2E\delta_B} \quad (36)$$

$$A_{eff} = \frac{Pl}{G} \left(\delta_C + \frac{11}{3} \delta_B \right) \quad (37)$$

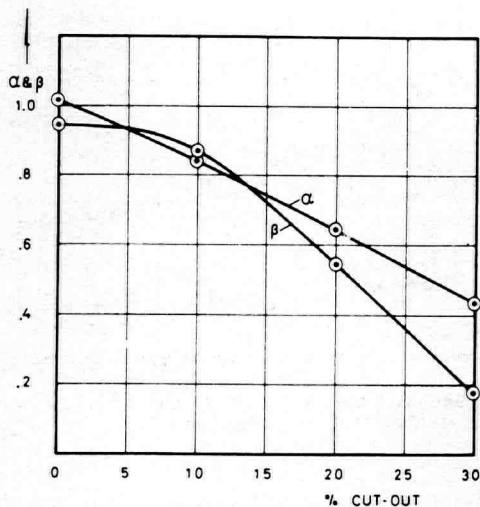


Fig. 31 Coefficients α and β as functions of percentage cut-out

The following notations have been employed:

- E = Young's modulus
- G = shear modulus
- P = loading applied along the height of the bulkhead
- l = characteristics span, see Fig. 30.
- I_{eff} = effective, or equivalent, moment of inertia
- A_{eff} = effective, or equivalent, shear area

The actual deflection curves of the lower edge of the bulkhead found by the finite element technique and by model test, could be represented by using efficiency factors for the cross-sectional area and for the moment of inertia of the following type:

$$\alpha = \frac{A_{eff}}{A} \quad (38)$$

$$\beta = \frac{I_{eff}}{I} \quad (39)$$

where,

- A = complete cross-sectional area of the intact bulkhead
- I = complete moment of inertia of the intact bulkhead

The values found for α and β are given in Fig. 31.

In addition to the basic loading given in Fig. 30, four other types of inplane loading of bulkhead models were investigated. The α and β values shown in Fig. 31 represent the different types of loading with a reasonable degree of accuracy.

Of course, the amount of cutout area does not constitute a unique parameter for the efficiency of various bulkheads. It has been found, however, that narrow elements between the cutouts contribute very little to shear rigidity. The evaluation of the in-plane stiffness of wash bulkheads and their actual design, is strongly dependent on cutout configuration and location, that is, whether this particular component is located in the center tank or in the

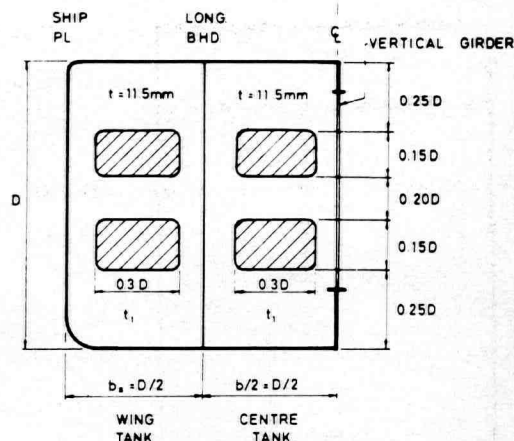


Fig. 32 Illustrative wash bulkhead configuration

wing tank. Furthermore, in view of the fact that wash bulkheads frequently will have to be reinforced with respect to plate thickness and stiffening in the lower region, from the bottom and up to $D/4$, say, it is also important to realize this effect upon the response and design characteristics of the wash bulkhead.

In order to demonstrate some of the effects associated with this, consider an idealized bulkhead in Fig. 32. The cross-hatched areas denote the principal openings, all plating above $0.25D$ is 11.5 mm, while that below may be varied as shown below.

Let us first consider the center tank domain:

Shear stiffness—Increasing the thickness, t , from 11.5 to 15 and 19 mm enhances the shear stiffness by 12 percent and 24 percent respectively.

Internal shear forces—Due to a force applied at the center line (from the center girder), the following takes place (in percent).

Region	Thickness, t , (mm)		
	11.5	15	19
Lower	26	51	56
Middle	23	21	19
Upper	31	28	25

Next, for the wing tank domain:

Shear stiffness—First, for $t = 11.5$ mm, the shear stiffness of the wing tank domain is only 72 percent of the corresponding value for the center tank. Moreover, the increase of t , from 11.5 to 15 and 19 mm, enhances the shear stiffness by 8 and 15 percent, respectively.

Internal shear forces—The shear force distribution between the longitudinal bulkhead and the ship plating may be described as follows (in percent).

Region	Thickness, t , (mm)		
	11.5	15	19
Lower	41	44	47
Middle	27	26	25
Upper	32	30	28

The design of the individual regions of the wash bulkhead is straight forward. Nevertheless, it is emphasized that the stability and combined stresses in the lower regions in certain instances, represent quantities which have been too lightly touched upon. Indeed, it must be kept in

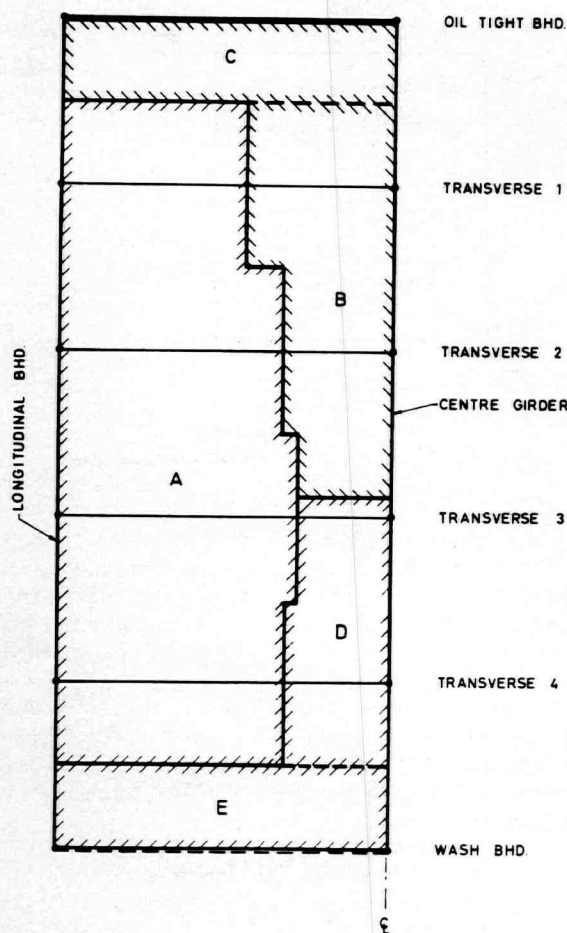


Fig. 33 Influence domains for one quarter of a center tank

mind that proper behavior of the bottom and deck structure is strongly dependent on adequate design of the wash bulkheads.

Furthermore, it must be noted that the design of the lower regions also is substantially influenced by the direct loads from the bottom longitudinals. These regions are frequently subjected to shear forces from domains *E* and *D* which are of the same order of magnitude. Manholes and similar large cutouts in the lower regions are frequently employed. They should, most certainly, be located with extreme care and preferably in locations of minimum shearing action. Stiffening should be provided to prevent overall and local buckling near cutouts, and where stiffener and girder loads are supported by the bulkhead structure.

Bottom Grillages in Tankers

With respect to the design of wash bulkheads and bottom transverses, it is frequently useful to consider a load distribution diagram as indicated by Fig. 33. This figure illustrates typical influence domains for one quarter of a center tank. The following explanation is pertinent: Domain *A* represents the "drainage area" for loads being carried to the longitudinal bulkhead via the bottom trans-

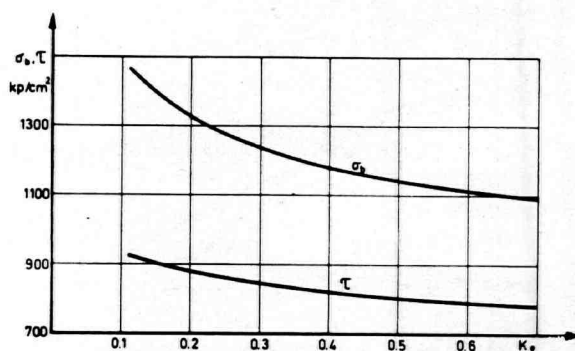


Fig. 34 Influence from wash bulkhead efficiency (k_e) on typical stresses in center tank bottom transverses

verses. Domain *B* carries to the oil tight bulkhead via the center girder, and domain *C* directly on to the same bulkhead. Essentially, loads from *B* and *C* are transported by the oil tight bulkhead to the longitudinal bulkhead. Similarly, zones *D* and *E* carry loads to the wash bulkhead, *D* via the center girder and *E* directly onto the wash bulkhead.

When it comes to the design of the transverse bulkheads, this picture should be kept in mind, and it is advisable to observe that the wash bulkhead has a considerable load domain. The picture is not materially altered when confronted with a system having three or five bottom transverses. Analogous diagrams are available for systems having one side girder on both sides of the center girder. Such a design would stress the transverse bulkheads substantially more, and would thus call for appropriate adjustment of the bulkhead scantlings.

The bottom transverses are quite susceptible to hold geometry and stiffness of wash bulkheads. For a typical large tanker having one wash bulkhead between adjacent oil tight bulkheads, five bottom transverses between bulkheads, and one strong center girder, Fig. 34 illustrates the variation of the maximum span bending stress and the maximum shearing stress at the bracket-toe close to the longitudinal bulkhead, as a function of shear efficiency factor, k_e , of the wash bulkhead. Normally, a value of $k_e = 0.3$ (relative the bulkhead being closed) would be considered on the low side.

Extensive systematic computations of bending moments and shear forces in the bottom of the grillage system of tankers show that both longitudinal girders and transverses will usually be subjected to an increase in the span and support bending moments and shear forces when a wash bulkhead with large cutouts is substituted for a rigid oil tight bulkhead. The situation is further aggravated when wash bulkheads are substituted for two neighboring rigid bulkheads.

In Fig. 35, tendencies are demonstrated for two different cases. In both cases, the length between supporting bulkheads is equal to the distance between the longitudinal bulkheads. The left-hand side of the figure shows the influence of various cutout areas in a wash bulkhead when every second bulkhead is a wash bulkhead. The right-hand figure shows the influence when there are two wash bulkheads for every oil tight bulkhead. Compensation for

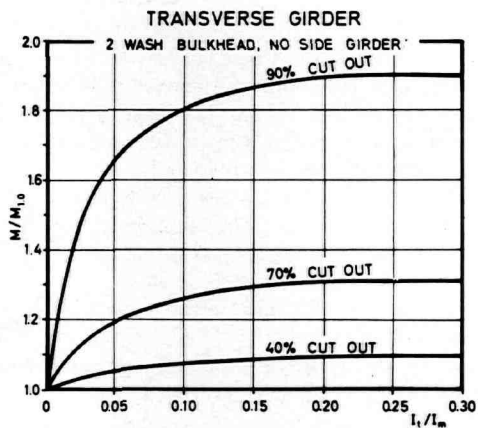
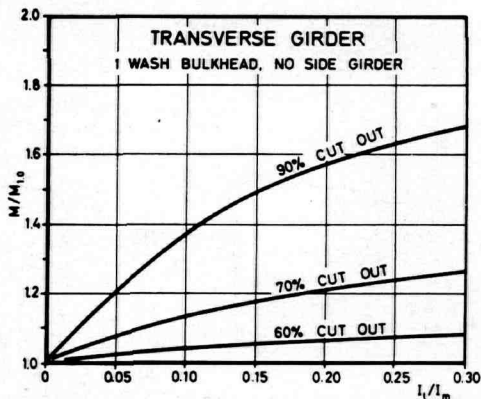
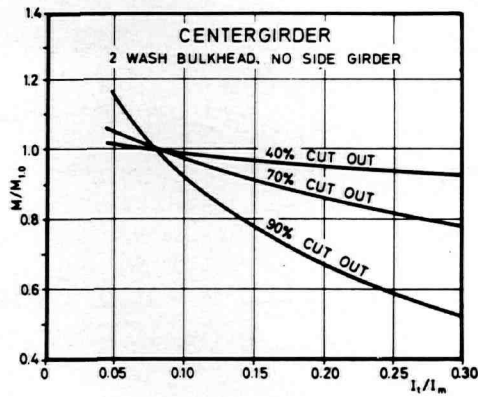
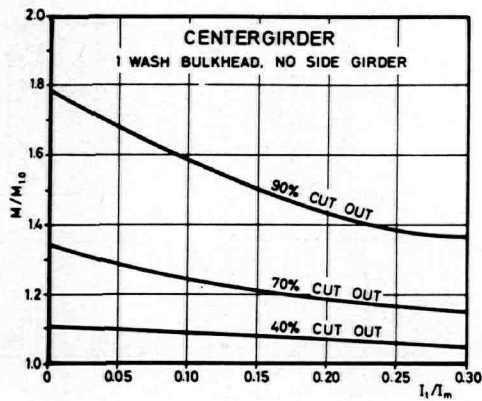


Fig. 35 Influence from wash bulkhead cut-out on the flexural response of center and transverse girders

cutouts in the form of increased plate thickness is not considered.

For the longitudinal girders, the increase in the span moment will be relatively smaller when the tank length to tank breadth ratio is increased. When two wash bulkheads are situated between the oil tight bulkheads and the distance between the oil tight bulkheads is more than 2.5 times the breadth of the tank, the span moment of the longitudinal girders will gradually be less than the span moment for the system with oil tight bulkheads only. In such cases, the transverses must carry the extra load due to the reduced shear carrying capacity of the wash bulkheads. The span moments in the transverses may in such cases be 30 to 60 percent larger than for the corresponding arrangement with rigid bulkheads of the oil tight type.

Even if the brackets on the longitudinal and transverse girders may take care of the moment peaks at the supports, our investigations clearly demonstrate that the brackets may have to be increased considerably in size to take care also of the very large shear forces near the supports. Adequate design in this case is a matter not only of a reasonable combined stress level with respect to rupture, but in most cases a question of adequate stiffening to prevent combined shearing and compression stresses to cause local buckling.

Current practice in the building of large tankers requires

that closer attention be devoted to shearing stresses than might have been the case in the past. Or, for that matter, the trend is definitely toward the obvious consideration of equivalent stresses by means of some appropriate yield criterion, for example, the von Mises-Huber-Hencky version. Thus, as a consequence of this, several cross sections and various locations in these cross sections, will sometimes have to be checked, and the development of building regulations becomes somewhat more laborious. In particular, regarding bottom transverses in tankers, it turns out that cross sections corresponding to maximum span moment (zero shear), a section in the immediate vicinity of the bracket-toe (adjacent to the longitudinal bulkhead), and a section at a possible discontinuity in the web plate thickness, will normally suffice for stress control.

For design purposes, it is important to notice that the shear forces in the bottom transverses, are remarkably invariant of flexural conditions around the whole boundary of the center tank. We have found that even substantially different fixities from those now assumed, will not give deviations in shearing forces greater than 5 percent.

Instability Phenomena of Some Girders

For the purpose of studying the effects of various stiffening arrangements, our Society carried out a program in-

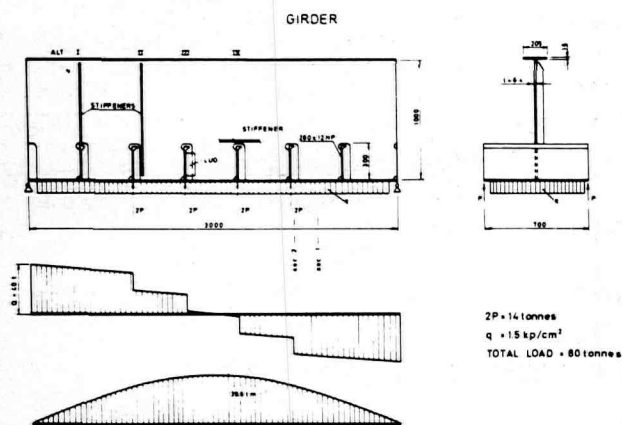


Fig. 36 Experimental model and loading scheme

volving several types of stiffening alternatives and notch details. These are shown in Fig. 36. The overall dimensions were common to all versions, with the exception that one experimental set of four girders involved a web thickness equal to 4.1 mm, the other set—also of four girders—entailed a thickness of 6.4 mm. The chosen dimensions reflect approximately a 1:2 scale of usual bottom transverses.

The various one-sided stiffening arrangements comprised the following alternatives.

Alternative I—All stiffeners were located vertically and welded directly to the longitudinals and the web.

Alternative II—All stiffeners were located vertically and immediately adjacent to the free boundary of the notches.

Alternative III—No stiffeners whatsoever, but all longitudinals were fitted with doublesided lug plates.

Alternative IV—One continuous horizontal stiffener immediately above the notches and no lug plates.

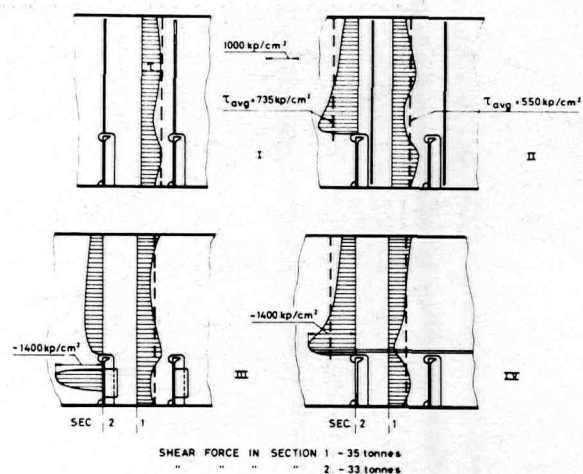
Typical shear force and moment diagrams are also contained in Fig. 36. The girders were all simply supported, and subjected to the simultaneous action of distributed loads, q , and concentrated loads, P . The ratio of the sum of the local loads to distributed loads were chosen to be 2.4. Pneumatic type rubber cushions acting on the bottom plating, provided good simulation of the direct bottom pressure. Independently of this, hydraulic jacks acted directly on the longitudinals. The details of the loading arrangement are depicted in Fig. 36.

The actual loading sequence was executed in suitable increments, always maintaining the required load ratio at the end of each application.

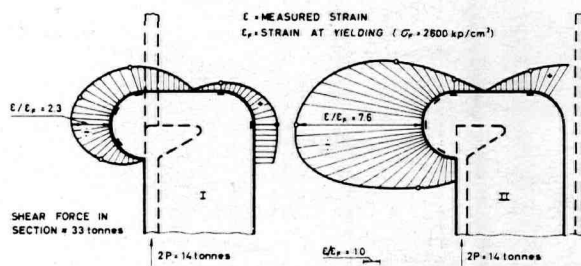
Two types of measuring devices were employed. Relevant strain distributions were recorded by means of double sided rosettes and simple gages, on the web plate and in the notches, respectively. Lateral deflections of the web plate were mapped by means of dial indicators. Recordings were made initially as well as during the entire loading program.

For each girder, loads were applied until the lateral deflections became very large (compared to plate thickness), and load application became hard to control.

Typical shearing stress distributions and notch stresses



a) DISTRIBUTION OF SHEAR STRESSES



b) STRAIN DISTRIBUTION AROUND OPENINGS

are given in Fig. 37. It is emphasized that corresponding cross sections in the four girder versions, carry identical quantities of shear forces. Thus the effects of different structural arrangements become readily apparent. It is important to notice the natural of the various distributions, and—in particular—that the diagrams between the notches display other characteristics than those directly above the notches.

For all cases involved, the average shearing stress on section 1 is 500 kp/cm^2 , which in turn has been indicated by a dashed line in Fig. 37a. Correspondingly, for section 2 we have 735 kp/cm^2 , while the maximum shearing stress is here of the order of 1400 kp/cm^2 .

Fig. 37b displays another advantage of using a stiffener directly to the longitudinal, namely to contain the plastic action of the notch. Clearly, with no stiffener welded directly to the longitudinal, the strains are considerably larger in magnitude. In all cases, however, it is quite obvious that extensive yielding may take place at certain locations of the notch contour.

From Fig. 37a, Alt. III, it is seen that the lug plate carries substantial shearing stresses compared to the girder web.

Referring to Fig. 36, it is mentioned that the maximum nominal bending stress is 900 kp/cm^2 .

Fig. 38a displays some typical buckling configurations.

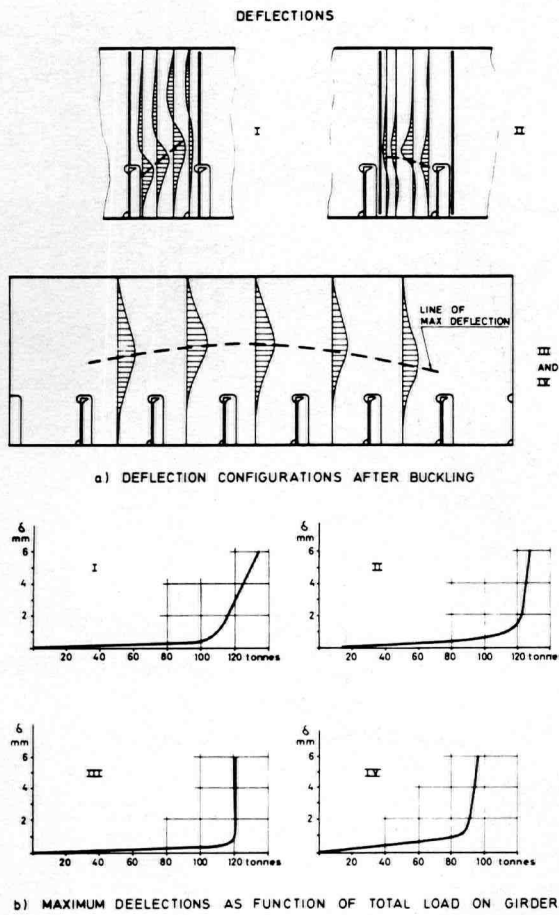


Fig. 38 Typical buckling configurations and response diagrams

Alt. I illustrates a shear buckle starting from that part of the free notch boundary which is in compression. Alt. II is provided with sufficient stiffening of the free boundary, and the stability phenomenon appeared as an almost horizontal buckle at all loaded notches simultaneously. Alt. III and IV showed a totally different buckling configuration than the former two. Here the whole web plate moved laterally as would be expected with the top flange as an effective restraint against lateral motion.

In Fig. 38b, characteristic deformation-load relationships are indicated. The curve belonging to Alt. I, refers to the general behavior of the region located adjacent to the left support of Fig. 38a. The other response curves, however, constitute more or less typical characteristics of the whole girder. Alt. II, III, and IV were essentially loaded to their ultimate capacity (load at drastic growth in displacements), while the ultimate strength of Alt. I was found to be considerably greater. Alt. I had a much more gradual increase in lateral deflections after initial instability than the other girder types. This must be attributed to a much more efficient stiffening of Alt. I. Indeed, it must be considered desirable to establish a design which manifests itself in proper warning, that is, that buckling phenomena are allowed to occur well in advance of the hazardous consequences of failure through ultimate collapse. The numerical results of Fig. 38 refer to a web thickness of 6.4 mm. Essentially the same tendencies were observed for girders having reduced thicknesses.

Discontinuities in Girders

We have also investigated various forms of structural

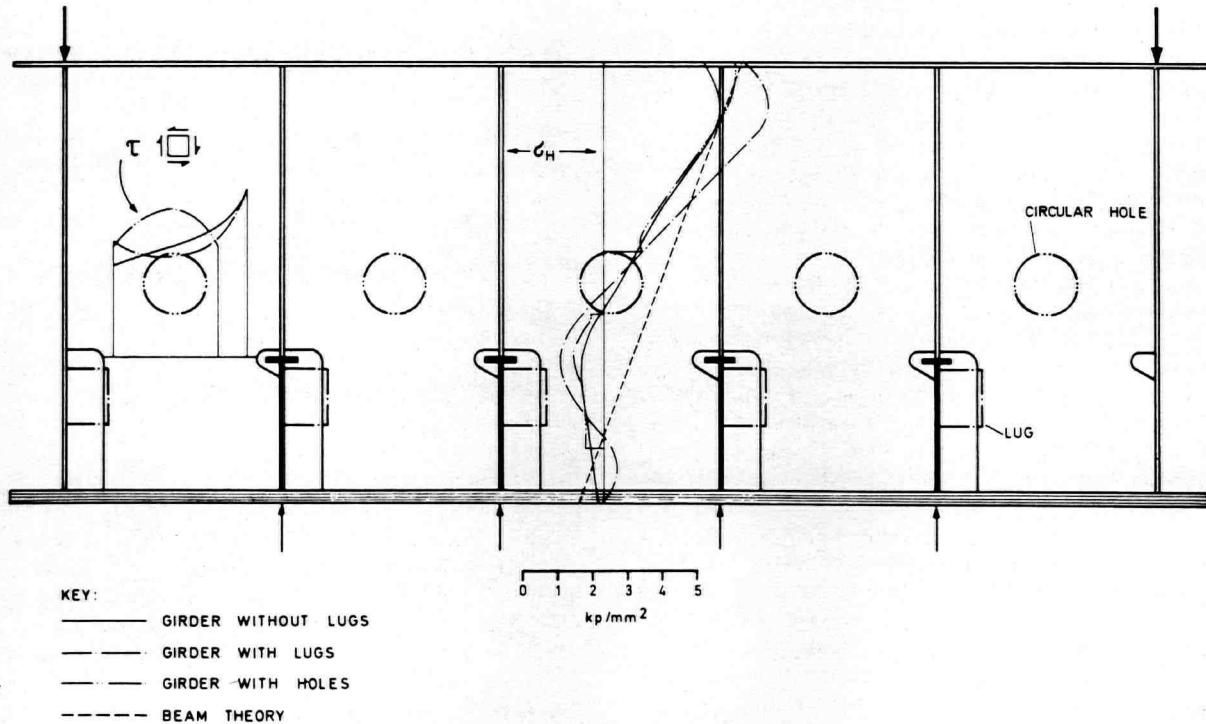


Fig. 39 Test results for an actual steel girder

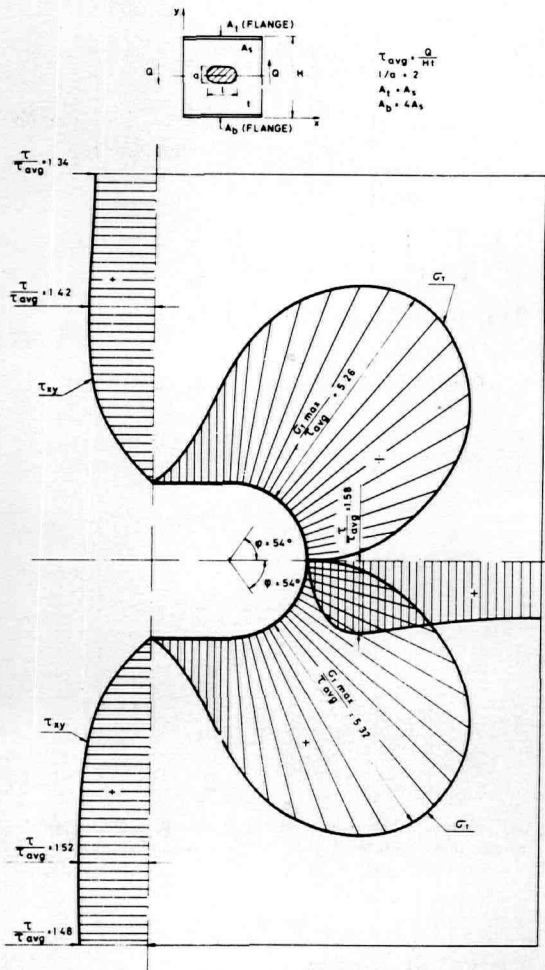


Fig. 42 Stress distribution for beam element in pure shear. Lying hole

of environmental loads which yield maximum compressive stresses, will be full draught and full center tank. For the two tie system, the forces due to such a combination may be written:

$$P_{tt} = (D/23) (31 + 33 D/23) s \quad (40)$$

$$P_1 = (D/23) (34 + 260/23) s \quad (41)$$

for the upper and lower, respectively. Results are in metric tons, provided D and s , the spacing of the frames, are taken in meters.

For a single tie system, we may write:

$$P = 56 (D/23)^2 (1 + D/23) s \quad (42)$$

Relative vertical displacements of the longitudinal elements will normally influence the direct forces in minor degree, but should nevertheless be included for design purposes.

It has been found that the above direct forces are almost independent of the tie cross-sectional area within the domain of practical interest.

In the bottom transverse in the wing tank, the shear

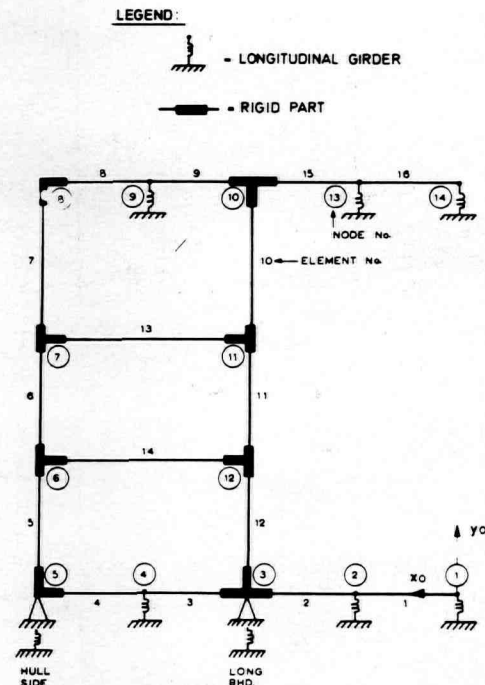


Fig. 43 Idealized computer model

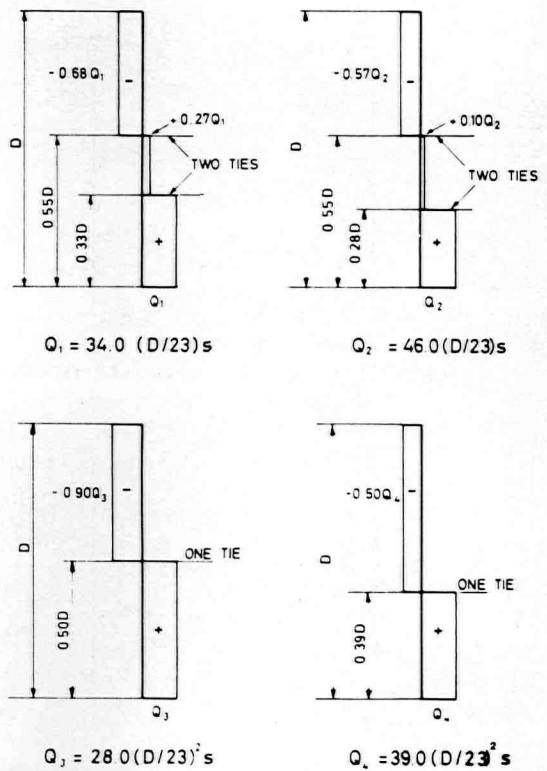


Fig. 44 Approximate shear force distribution in vertical girder on hull plating due to full center tank. $Q = 10^4$, $x = L/4$. Forces in metric tons

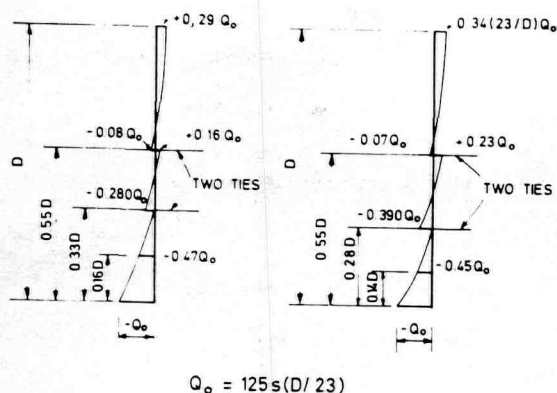


Fig. 45 Approximate shear force distribution in vertical girder on hull plating due to full draught. $Q = 10^{-4}$, $x = L/4$. Forces in metric tons

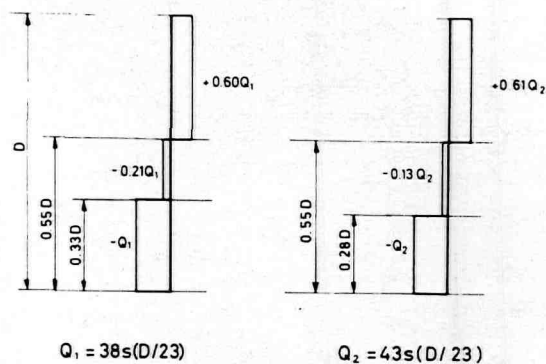


Fig. 47 Approximate shear force distribution in vertical girder on longitudinal bulkhead due to full draught. $Q = 10^{-4}$, $x = L/4$. Forces in metric tons

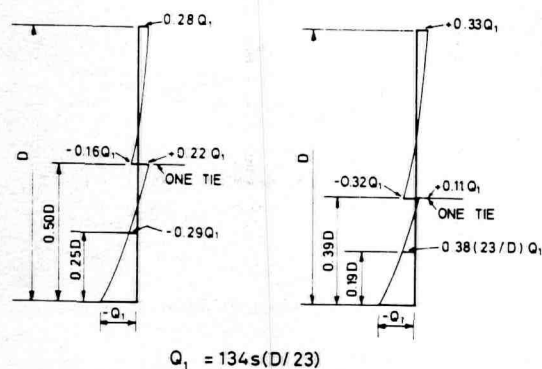
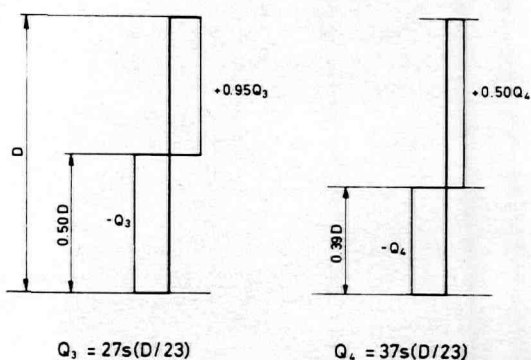


Fig. 46 Approximate shear force distribution in vertical girder on longitudinal bulkhead due to full wing tank. $Q = 10^{-4}$, $x = L/4$. Forces in metric tons



forces due to the combination of full draught and full center tank may be given by:

$$Q_H = (140b_s/11.5 - 29b/23) (D/23)s \quad (43)$$

$$Q_L = (-88b_s/11.5 - 29b/23) (D/23)s \quad (44)$$

indexes H and L indicates the hull side and the longitudinal bulkhead side, respectively. The quantities b_s and b denote breadth of wing tank and centre tank, respectively.

Now, due to a unit displacement of the longitudinal bulkhead, we may approximately obtain the following additional shear force (metric tons) in the bottom transverse given by,

$$Q_1 = 0.017(D/23)(EI/b_s^3)/(1 + 0.0031I/(A_s b_s^2)) \quad (45)$$

where

- E = Young's modulus, kp/cm^2
- I = moment of inertia of bottom transverse, cm^4
- A_s = effective shear area of bottom transverse, cm^2
- b_s = breadth of wing tank, m
- D = depth molded, m

Furthermore, a unit displacement of the center girder relative to the hull side, may give a shear force approximately equal to,

$$Q_2 = -25 (23/b)^3 \quad (46)$$

in metric tons provided b is taken in meters.

For the top transverse in the wing tank, it is interesting to notice that the combination of full draught and full

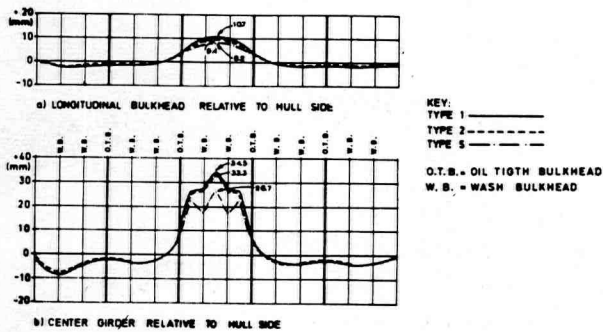


Fig. 48 Relative displacements in mm. Full draught and one empty center tank ($l_c = 0.18L$)

center tank yields essentially no shear. A unit displacement of the longitudinal bulkhead relative to the hull side yields the following,

$$Q_3 = (50 + 68 \cdot 10^{-7} I) (11.5/b_s)^2 \quad (47)$$

where I represents the pertinent moment of inertia of the top transverse.

Figs. 44 and 45 demonstrate the shear force vibration for one and two tie systems in the vertical girder on the ship side. Regarding two tie systems, the lower and upper regions of the diagrams yield good values, while the middle part may give some inaccuracies. The latter region is, however, rarely of particular interest from the standpoint of structural design. The figure does not include the effects due to relative vertical displacements of longitudinal bulkhead and ship side.

In Figs. 46 and 47 we have shown the shear forces in the vertical girder on the longitudinal bulkhead due to wing tank filling and full draught loading. Affects due to relative displacements have not been included in these diagrams.

The influence of the relative displacements between longitudinal girders, longitudinal bulkheads, and ship sides were investigated theoretically, treating the ship structure between the end bulkheads in the cargo tank range as a continuous grillage structure. One sample of the results, showing relative displacements for the ship in a fully loaded condition, but with one empty center tank, is shown in Fig. 48.

We found that for the case of strong up-lift in one center tank section, the zone of influence on transverse displacements is of the same local character.

A considerable change in the moment of inertia of the longitudinal bulkhead and hull side does not have any substantial affect on the local response picture, see comparison of Type 1 and Type 2 in Fig. 48.

Doubling the shear stiffness of wash bulkheads tends to reduce the maximum relative displacement by approximately 25 percent, see comparison of Type 1 and Type 5 in Fig. 48.

Increasing the shear stiffness of web frames by 25 percent, tends to reduce the maximum relative displacements by 8 to 3 percent, for the longitudinal bulkhead and the center girder, respectively.

Even a considerable change in the stiffness of the center

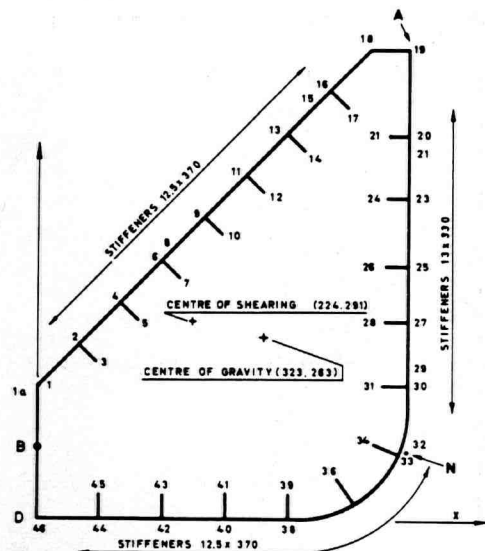


Fig. 49 Typical bilge tank of a bulk carrier

girder will have only a slight affect on the displacements transversely.

A reduction in the length of the empty tank by a certain amount will lead to a corresponding reduction in the relative displacement.

One pair of empty wing tanks, all adjacent tanks being full, will cause only negligible relative displacements between ship side and longitudinal bulkhead.

On the bases of the results of this investigation, it is possible to conclude:

1 Bending moments are quite sensitive to changes in geometry and cross sectional data. Shear forces are somewhat less influenced by such variations. The above is particularly true for relative displacement type loadings, while both moments and shear forces are relatively independent of cross-sectional data when subjected to distributed loads alone.

2 Considerable variation in the cross-sectional area of ties has an almost negligible effect on the stress resultants.

3 A reduction of the full web area by up to approximately 30 percent, give only a minor influence on the stress resultants, arising as a result of distributed loads.

E. Strength Problems Concerning the Double Bottom

Strength calculations of double bottoms are of particular significance in connection with the design of large bulk carriers. The bottom structure is supported by transverse bulkheads and the ship sides. The flexural restraint offered from a usual transverse bulkhead is small, except in cases of having doubleplated bulkheads. Similarly, the ship plating will normally provide only a small amount of flexural restraint on the double bottom structure in the transverse direction. For all practical purposes, the above flexural restraints may be neglected. However, a large bilge tank along the ship sides will contribute substantially to the flexural restraint acting on the double bottom. Fig. 49 depicts such a bilge tank. It is to be noted that the

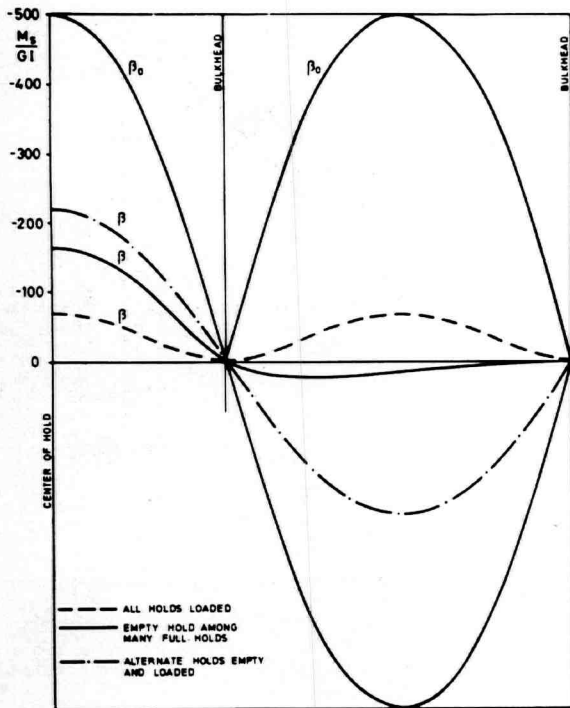


Fig. 50 Angle of twist for various loading arrangements

median plane of the double bottom and the ship's plating intersect at point N .

To take care of the strength analysis of double bottom structures in connection with approval of drawings, we usually make use of computer program which is based on the following assumptions:

1 The double bottom is assumed to consist of a system of intersecting beams. Cross-sectional data are given in such a way that torsional stiffness and the in-plane shears force system in the continuous plate structure is taken into account.

2 The continuous double bottom structure is supposed to be elastically supported at the transverse bulkheads. The elasticity in the transverse bulkheads is mainly due to shear deflection.

3 We usually assume the ship sides to form a continuous and nonyielding support and that the bilge tank provides an elastic rotational restraint on the bottom system.

For ordinary design purposes, this procedure may not always be very helpful for the designer at the design stage. Ordinarily, the designer likes to have recourse to a method in which the parameters are not implicitly given. We have therefore tried to formulate an explicit method which may give the designer a first approximation to his double bottom structure.

In what follows, we shall briefly discuss some of the particular effects due to the torsional rigidity of the bilge tank. Usually its torsional rigidity is much larger than the Bredt-type torsional rigidity of the single box beams which make up the double bottom grillage.

If we consider Fig. 49, we will notice that a bilge tank on the assumptions given above can only be displaced horizontally at point A , and vertically only at point B . This

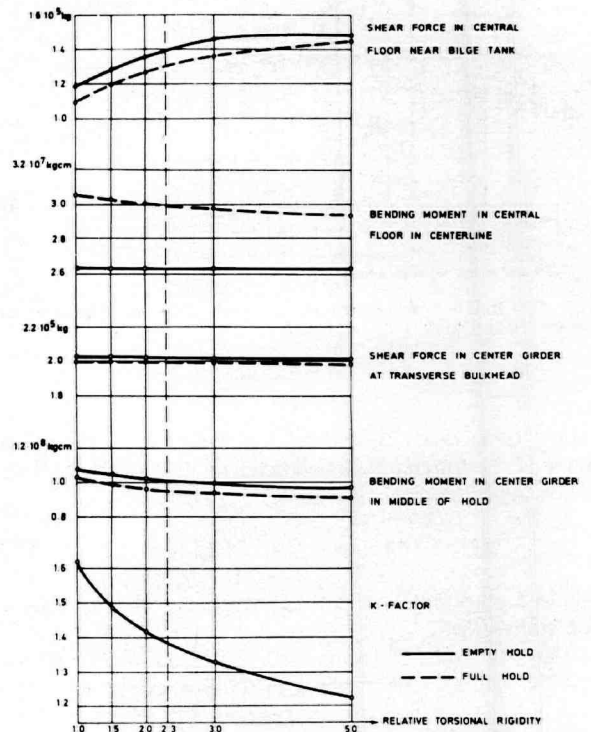


Fig. 51 Various response characteristics as a function of the torsional rigidity of the bilge tank

means that a bilge tank must rotate about a point N which is not the shear center of the tank. In order to investigate the warping effect on the structural response—assuming only transverse loads to be relevant—consider the following fourth-order differential equation,

$$\frac{dM}{dz} = GI_T \frac{d^2\beta}{dz^2} - EC \frac{d^4\beta}{dz^4} \quad (48)$$

where:

- β = angle of twist
- z = longitudinal coordinate
- M = torque about the z -axis
- GI_T = torsional rigidity
- EC = warping rigidity

Based on this equation, we have investigated the influence of the torsional stiffness of the bilge tank on the strength of the double bottom for some practical cases, including loading of every second hold, loading of all holds, and one empty hold among a large number of loaded holds.

To investigate the torsional rigidity of the bilge tank, we assumed the applied torque to vary linearly along the tank. Upon differentiating equation (48), it may be shown that the following solution is obtained,

$$\beta = C_1 \sinh \alpha Z + C_2 \cosh \alpha Z + C_3 Z^2 + C_4 Z + C_5 \quad (49)$$

where:

$$\alpha = \sqrt{\frac{GI_T}{EC}}$$

By selecting the boundary conditions carefully, it is possible to find the angle of twist.

In Fig. 50 is shown the relative torsional rigidity of a bilge tank for three different conditions of loading of the holds. It is seen that in all cases the torsional rigidity is considerably larger than found by assuming the bilge tank to rotate about its shear center, that is, the warping constraint is substantial.

In Fig. 51, the influence of the torsional rigidity of the bilge tank on shear forces and bending moment in the double bottom is shown. When holds are alternately loaded, it is seen that the bending moment in the center girder and in the transverse floor in the center of the hold is very little influenced by the torsional stiffness of the bilge tank. The same holds for the shear force in the center girder near transverse bulkheads. The shear force in the central transverse floor near the bilge tank is, however, considerably increased by increasing torsional rigidity of the bilge tank. The so-called K-factor, denoting the part of the load of the double bottom which is transferred to the transverse bulkheads, is markedly influenced by the torsional rigidity of the bilge tank.

Assuming the loading on the double bottom to be composed of the static difference of loading in still water due to cargo on the inner bottom and hydrostatic pressure on the other bottom, and the additional statistical loads due to the acceleration forces created in the cargo as well as the additional hydrostatic pressure caused by a relative motion of the ship and the wave surface, we have found it reasonable to accept bending stresses in the transverses up to 1500 kp/cm^2 in the transverse direction at the probability level of 10^{-8} . This corresponds to about 1200 kp/cm^2 for the still water loading alone.

The corresponding shear stress on the net area of transverses may be 1100 kp/cm^2 , corresponding to 900 kp/cm^2 for still water loading only.

Usually it would be difficult to maintain buckling stability of an ordinary double bottom structure at the level of more than about 2000 kp/cm^2 in ordinary ship steel having a yield point of 2400 kp/cm^2 . Even if the double bottom may have considerable residual strength after a buckling failure in a small region, it is necessary to ascertain that the stress levels in such regions do not exceed the limit of 2000 kp/cm^2 with the probability of 10^{-8} .

With such a low probability as 10^{-8} , it would not seem unreasonable to let the total combined stresses due to longitudinal of the ship hull girder (primary bending) and local bending of the double bottom as a plate (secondary bending) approach the yield point of the material.

A reasonable amount of corrosion allowance must be observed. Also the tertiary bending stresses of the plating in the outer and inner bottom have to be taken into account. When such extreme loading cases as indicated above are used as a basis for the stress calculation, it is reasonable to accept local yielding of the plating material when calculating stresses. Under such extreme loads, the plating will deform in such a way that a considerable part of the local loads are carried by membrane forces in the plating.

Certain compensations will have to be considered for

the inner bottom with respect to grab and truck loading, and — in view of containerized transport — for concentrated loads due to container stacking.

F. The Longitudinal Hull Girder Section Modulus

The longitudinal hull girder bending forces are all of a statistical nature. The statistics of the wave bending and shearing forces have been treated in some details. The still water loading has a statistical distribution which is defined by rather narrow bands of bending moments and shearing forces, for instance one band describing the loaded condition of the vessel and another relatively narrow band describing the ballast condition. This is usually the case for tankers and bulk carriers. Sometimes the narrow bands corresponding to the ballast and the loaded condition may melt together in one narrow band. In other cases, as for instance for general cargo ships, the still water loading may be given by a fairly broad spectrum.

In addition to the wave and still water loading, account should also be made of slamming stresses, thermal stresses, propeller thrust forces, surging stresses, and so forth. It is obvious that it is rather difficult to include all these loads in a rational manner, superimposing the loads statistically with their right phase angles.

In connection with fatigue damage, we are interested in the cumulative effect of all these loads; in connection with the ultimate strength, we should base our calculations on an extreme load; and in connection with the probability of brittle fractures, an extreme load level should be defined in connection with a low temperature level. It seems that all fractures in steel ships may be referred either to plastic buckling, brittle fracture, high stress or low stress fatigue failure.

In connection with a brittle fracture, the frequency of the wave bending moment is usually so small that it may be regarded as a quasi static moment, and may be directly added to the still water bending moment.

We have determined the wave bending moment occurring with the probability of $Q = 10^{-8}$ on the North Atlantic route as a reasonable extreme wave bending moment for our ships. In this connection, it should be mentioned that statistical calculations of the type used here tend to give the worst part of a ship route a rather heavy influence on the statistical results. A level of probability corresponding to $Q = 10^{-8}$ on the North Atlantic route, will according to our information, correspond to a probability level $Q = 10^{-10}$ to $Q = 10^{-11}$ for the entire ship population with length greater than 100 m. A probability level $Q = 10^{-11}$ corresponds to about 50,000 ship years.

Disregarding brittle fracture, it would be reasonable to define the extreme collapse load on the basis of the sum of the still water bending moment which is exceeded with a probability of say 1 percent, and the extreme wave load as defined above. Since the still water bending moment usually has a rather narrow band, the probability level chosen for this part will have a comparatively small influence.

On the tension side of the structure, stresses might, in such an extreme case, be allowed to approach the yield

limit of the material, with a certain safety factor placed on the structure to allow for deduction due to corrosion and inaccuracies in calculating the strength of the structure.

On the compression side of the structure, the possible influence of local pressure should be regarded when considering the buckling collapse of the structure.

As shown by Caldwell [26], the ultimate moment of resistance of the hull girder, making allowance for buckling, is given by:

$$M_u = \sigma_y AD \left[\alpha_D \beta_D \gamma + 2\alpha_s \left\{ 1 - \gamma + \gamma^2 \frac{(1 + \beta_s)}{2} \right\} + \alpha_B (1 - \alpha) \right] \quad (50)$$

in which the position of the equal area axis is defined by:

$$\gamma = \frac{g}{D} = \frac{2\alpha_s + \alpha_B - \alpha_D \beta_D}{2\alpha_s (1 + \beta_s)} \quad (51)$$

In these equations, α indicates a portion of the total cross-sectional area A , β indicates an efficiency factor for the structure, indexes D , S , and B refers to deck, side, and bottom, respectively. Eq (50) and (51) assume that a plastic hinge may be fully developed across the midship section.

Little information is available on the efficiency factor β_D and β_B for ordinary tankers and dry cargo ships. From calculations it appears that the efficiency values in buckling equal to 0.8 should be obtained on the net section after deduction for corrosion and water. An efficiency factor $\beta = 0.9$ would seem reasonable on the tension side.

The efficiency factor on the bottom side will usually have to be adjusted for secondary bending of the double bottom. Unless large amounts of cargo are carried on deck, it seems that little further adjustments would be necessary for the deck efficiency factor.

The resulting midship cross section should then satisfy the following condition:

$$M_u \geq M_w^{(-11)} + M_{sw}^{(-2)} \quad (52)$$

where the quantity inside the parentheses is the logarithm (base 10) of the probability of exceedance, and the subscripts u , w , and sw denote "ultimate," "wave," and "still water," respectively.

It is much more difficult to define rational stress level with respect to brittle fractures. We have, however, reasonable guidance in the stress levels defined for present-day large ships which have been successful with respect to brittle fracture considering the material used in ships nowadays. The required longitudinal sectional modulus according to the rules of our Society is,

$$W = \frac{M_w^{(-6)} + M_{sw}^{(-2)}}{\sigma_{b.f.}} \quad (53)$$

where $\sigma_{b.f.}$ denotes the allowable bending stress with respect to brittle fracture.

The nominal bending stresses based on ordinary ship steel with a yield stress of 2400 kp/cm² is given by:

	Hogging Condition	Sagging Condition
Deck	1250 kp/cm ²	1350 kp/cm ²
Bottom	1350 kp/cm ²	1250 kp/cm ²

The comparatively low stress level chosen must be regarded in relation to the probability level and to the additional stresses which may be superimposed. Essentially, brittle fracture will normally start from micro stress concentrations superimposed on a macro stress concentration, such that the total stress level at the point of possible initiation of brittle fracture might be rather high. In this connection, reference is made to [28] which showed that the average stress at fracture was only 200 kp/cm² for specimens with fatigue cracks, and loaded at the temperature between -40 deg and -10 deg C.

When materials of the fine-grain type with higher yield point and with correspondingly better properties with respect to brittle fractures are used in hull construction, it should be possible to disregard brittle fracture in connection with the definition of midship section modulus. So far, our experience with high yield point materials is limited but we have accepted an increment in the allowable stress level practically proportional to the yield point of the material.

Experience has shown that it is necessary to limit the stresses in the various ship components also with respect to fatigue. With the macro and micro stress concentration factors presently accepted in ship structural design, with the local secondary and tertiary stress levels adopted, and with the knowledge of additional stresses to which a ship is normally subjected, it is rather difficult to establish rational criteria for a midship section modulus which is meant to take care of the fatigue problem. However, it seems reasonable to assume that the wave bending moment variations during the life of a ship should play an important role in defining the minimum section modulus with respect to fatigue. Fatigue tests with built up test specimens show that the mean stress level may be rather important for the cumulative damage in fatigue contrary to the opinion held earlier. From the scarce material available with respect to fatigue failure it seems that the allowable total stress may be given by,

$$\sigma = \sigma_e (1 + \gamma \sigma_m / \sigma_e) \quad (54)$$

where,

σ_e = endurance limit

σ_m = mean stress

γ = parameter pertaining to the mean stress influence

Then it follows that the sectional modulus with respect to fatigue is given by,

$$W = \frac{[M_w^{(-4)} + M_{sw}^{(-2)}] \left(\frac{\delta}{\sigma_e} \right)}{\left[1 + \gamma \frac{M_{sw}^{(-2)}}{M_w^{(-4)}} \right]} \quad (55)$$

where δ is a characteristic stress concentration factor. It seems reasonable to choose $\gamma = 2/3$ and $\delta \approx 2$.

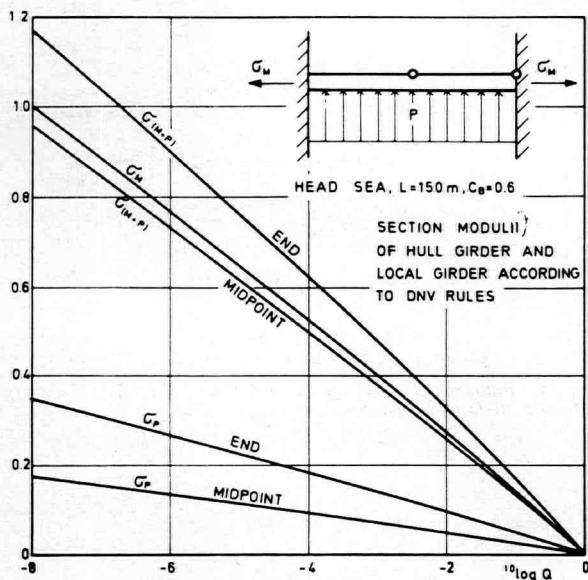


Fig. 52 Long term distributions of wave induced stresses in a bottom longitudinal amidships exposed to loads from longitudinal bending moments and local external water pressures

G. Stresses in Members that Are Simultaneously Exposed to Different Types of Loads

Most members in the ship structure are simultaneously exposed to different types of static and dynamic loads. Let us, for example, consider a longitudinal in the bottom of a ship. This member is exposed to longitudinal loads associated with the overall longitudinal still water and wave bending moments in the hull girder. It is also exposed to transverse loads due to external and internal water pressures of both static and dynamic nature.

It is common to handle the stresses set up by such loads separately and add the different types of stresses in a statical way. However, the dynamic loads do not reach their maximum values simultaneously and a static summation with no regard to the phase angles between the different types of loads can therefore lead to considerable errors.

It is possible to find the statistical distribution of combined stresses by calculating the transfer functions (see Part I.B) for the stresses due to longitudinal loads and for the stresses due to transverse loads. These transfer functions can be obtained from the transfer functions of longitudinal bending moments and local water pressures respectively. By combining the transfer functions for the different types of stresses with due regard to the phase angles, it is possible to obtain the transfer functions for the combined stresses.

Such a transfer function can then be used to obtain the long term statistical distributions of the stresses according to the principles described in Part I.B.

An example of a result obtained from this type of analysis is shown in Fig. 52. This figure shows the long term distributions of stresses at the end and at the midpoint of a bottom longitudinal amidships exposed to loads from longitudinal bending moments and local external water pressures. The longitudinal is supposed to have

clamped ends. As seen in the figure, the combined stresses are rather different from the static sums of the separate stresses. This shows that it is necessary to consider the phase angles between the different types of loads and carry out an analysis according to the principles mentioned above. We are now working with a systematic analysis of local stresses according to these principles, where also internal dynamic loads due to accelerations are taken into account.

H. Slamming on the Bottom Forward

Slamming is a well-known phenomenon associated with extreme motions of a ship in rough seas. When the fore-foot of a ship in an emerged condition again immerses such that the relative entrance velocity between ship bottom and sea surface exceeds a certain threshold value, the forward bottom sustains a heavy impulsive pressure from the water.

The threshold velocity seems to be approximately constant for all ship lengths when it is given in a nondimensional form.

The magnitude of the hydrodynamical impact pressure caused by a slam is a function of the relative velocity between bottom and sea surface and the local form and constant. The pressure may be given in the following form:

$$p = 2 c \overline{RV}^2 \quad (56)$$

where:

p = pressure head in meters

c = local form constant

\overline{RV} = relative velocity between wave and bow at instant of slamming, in m/sec

The local form constant is given by

$$c = fk \quad (57)$$

where f may be taken as a local form factor and k is a constant taking the hydroelastic and other responses into account.

The local form constant multiplied with twice the second power of the relative velocity between the considered part of the bottom and the sea surface shall describe the pressure distribution along the forebody of the ship.

When comparing two ships with equal motions, the difference in local form constant shall correspond to the difference in pressure.

By intuition, one would feel that the hydrodynamical impact is reduced in an elastic structure as compared with a rigid one. Meyerhof [21] shows that this is not always the case with a wedge shaped body with an elastic bottom plate. If the pressure impulse on the plate is long compared to the cycle of the free oscillations of the plate, the deformation follows the impulse very well. However, the upward acceleration of the plate relative to the body is negative already after the first quarter of a vibration cycle, and in turn, the relative velocity between the plate and the sea surface is augmented.

This means that the pressure may be higher on an elastic bottom than in the case of a rigid one in certain

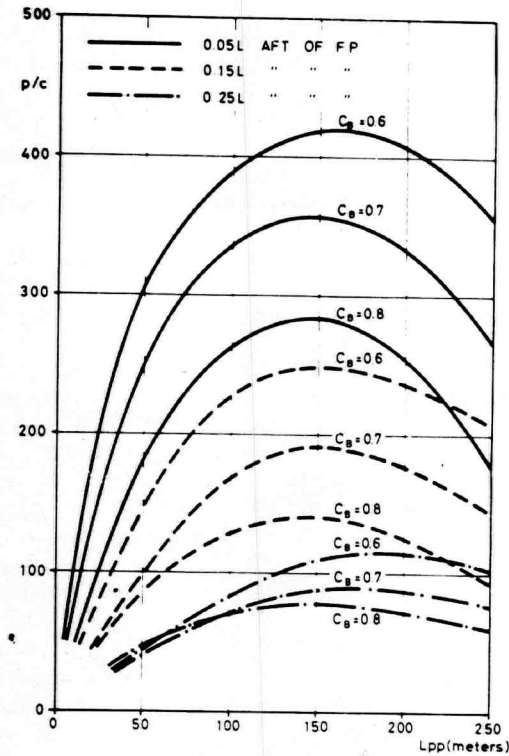


Fig. 53 Slamming parameter p/c on Series 60 in head seas

phases of the impact process. The magnification of the bottom pressures experiences in an elastic bottom with low natural frequency, as compared to those found in a solid bottom, can only be prevented when the free oscillations of the bottom are very slow compared to the slamming impulse which may last from 0.06 to 0.12 sec. However, the magnification factor for ordinary ship structures does not seem to be very great and the statistical way of calculating the plate thicknesses from the pressures obtained seems to be satisfactory because the natural period of the plates is much shorter than the duration of the impulse.

The long term distribution Q (p/c) of the quantity p/c may be calculated according to the principles described before. Variables of great importance for the relative velocity $R\bar{V}$ are ship length, form, speed, draught, and mass distribution. The p/c -ratio is also strongly dependent on speed reduction in heavy weather. In our investigations we have used a regression analysis of empirical data to obtain reasonable criteria for speed reduction in heavy weather. The condition chosen means that a master will reduce speed if the probability of slamming or bow submergence exceeds a certain threshold function which increases when the ship speed decreases.

The influence of the various parameters on the long term response is difficult to describe in a simple formula. In Fig. 53 we have shown the p/c -values as function of the ship length and block coefficient and with the different stations aft of the forward perpendicular as a parameter. The p/c -values shown correspond to a probability level of $Q(p/c) = 10^{-6}$.

The curves in combination with increased plate thick-

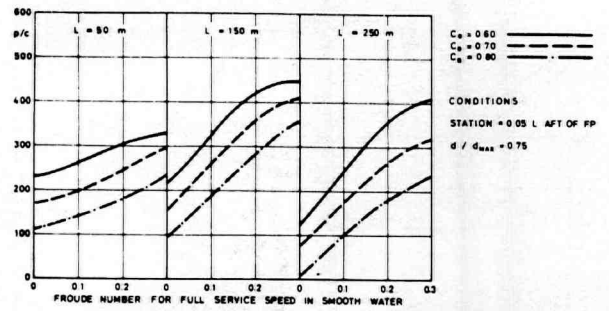


Fig. 54 Influence of ship speed and block coefficient on slamming parameter p/c on Series 60 in head seas

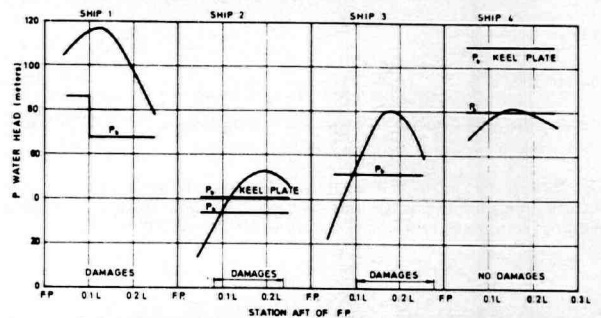


Fig. 55 Comparison between calculated slamming pressures and pressures causing initial yield at midpoint of plate on some ships with and without damages due to slamming ($d/L = 0.040$, $Q = 10^{-6}$)

nesses usually applied for bigger ships clearly demonstrate why ships with length above about 200 m are rarely exposed to forward bottom damages. This may also be due to the relatively greater load and ballast draughts of such vessels as well as their relatively smaller radii of gyration. Ships smaller than about 100 meters in length seem to experience smaller slamming pressures than they should statistically if they had experienced the sea states described as North Atlantic average. Usually such smaller ships may have recourse to sheltered waters under heavy weather conditions. Also the master will be more inclined to select a proper speed reduction and shift his heading under severe conditions. It may therefore be reasonable to reduce the calculated values for small ships.

The influence of the ship speed on the p/c -value is illustrated in Fig. 54. The curves shown have been adjusted for speed reduction in heavy weather. A correction factor taking the influence of the speed into account, may be given in the following form:

$$C_1 = 1.0 + (Fn - 0.2) \left[\frac{L}{200} + 10C_B - 5(1.1 - x/L) \right] \quad (58)$$

The influence of the mass distribution on the slamming pressures is comparatively small when speed reduction in heavy weather is taken into account. For a ship with length 150 m, a variation of the radius of gyration from 0.22 to 0.28 may give a 10 to 15 percent increase in the p/c -value.

The influence of the draught of a ship on the p/c -value may be taken into account by a correction factor C_2 of the type:

$$C_2 = \frac{8}{1000 (d/L)^{3/2}} \quad (59)$$

As the local form constant we have found the most appropriate factor for practical use to be:

$$f = \frac{1}{t_g \beta} \quad (60)$$

where β is the slope angle of the bottom of a section measured from the keel to a point at the side situated at a distance of $0.15 d_{\max}$ above the base line. The formula for calculating the bottom pressure will then be given by:

$$p = kf(p/c) C_1 C_2 \quad (61)$$

According to Ochi [25] the local form factor c equals $0.0325 \text{ (kp/cm}^2\text{)}/(\text{m/s})^2$ for a station situated $0.1 L$ aft of *F.P.* on the *Mariner* model used in his tests. Using this value, we get $k.f = 0.0325$ according to equation (57). At this station $k = 1.55$ according to equation (60) and therefore we get $f = 0.0325/1.55 = 0.021$. However, the values of p/c given in Fig. 53 refer to head sea and shall be multiplied with $2/3$ to obtain the corresponding values assuming that the ship travels equally long time in all directions relative to the waves. We include this correction in f and obtain $f = 0.021 \cdot 2/3 = 0.014 \text{ (kp/cm}^2\text{)}/(\text{m/s})^2$.

The elastic and plastic response of the bottom to impulsive loads of the slamming type has not yet been fully clarified. It seems that bottom damage due to slamming is slowly developing as a result of a series of slams and that one single slam is rarely responsible for bottom damage.

The damage starts with the information of plastic hinges in the bottom plating, in the stiffeners and may be as local buckling in the floors and girders. The ultimate load before failure of plane stiffened panels may be about 3.0 to 3.5 times higher than the load causing plastic hinges in the stiffeners.

Provided that the stiffeners and the stiffener supports do not collapse, the bottom plating will develop larger membrane forces after formation of plastic hinges such that the ratio between the collapse pressure and the pressure causing plastic hinges in the plating will be higher than the ratio 3.0 to 3.5 obtained from the stiffeners.

With a probability level of $Q(p/c) = 10^{-6}$ which means that the maximum pressure statistically is obtained once in about 0.5 ship years, it is acceptable to approve of rather high nominal bending stresses in the plating.

Basing on tests and experience we have established the following requirements to the bottom plate thickness t :

$$t = k_1 a \sqrt[3]{\frac{2400 p}{\sigma_y}} \quad (62)$$

where σ_y is the yield stress.

A constant dependent on the allowable stress in the plate and the length-breadth ratio a/b of the rectangular plate element k_1 is given in the table below:

a/b	1.0	0.9	0.8	0.7	0.6	0.5	0.4
k_1	2.57	2.83	3.01	3.14	3.20	3.23	3.26

It should be noted that the yield point and the elongation are the more important properties of the material in connection with bottom damage forward. It would definitely pay to use material with higher yield point in the slamming area, both for plates and stiffeners.

Since the middle of the fifties, our Society has strongly advocated the use of intermediate frames in the flat bottom forward. Our experience with this type of design has been extremely good, but the intermediate frames should be continued through girders and floors.

When dimensioning these frames, we have found it reasonable when using a probability level $Q(p/c) = 10^{-6}$ and applying a degree of fixation of 0.7 at supports, to accept a stress level corresponding to $\sigma = \sigma_y/1.5$ in tension. The section modulus requirement will then be given by:

$$W = 10000 \frac{pab^2}{\sigma_y} \quad (63)$$

This corresponds to a pressure causing full developed plastic hinges in the stiffener about four times higher than the design pressure, and a collapse load about twelve times as high. The load causing fully developed plastic hinges in the stiffener would, according to our statistical theories, be experienced about once in 5000 ship years. The local permanent deflection would in this case be about $1/270$ of the stiffener span.

Brackets have to be fitted to the bottom frames at supports.

It is of course also essential to provide the necessary strength of the double bottom system as such at the forward end of a vessel. In this connection it should be mentioned that the indicated pressure distribution corresponds more to the envelope of all slamming pressures than to one single particular slam.

A somewhat lower pressure than the one indicated above may be used when dimensioning the double bottom structure forward. Usually no difficulties are experienced in providing the added strength necessary at the forward part of the ship and to secure that the local forces are transferred to the ship girder in an efficient way.

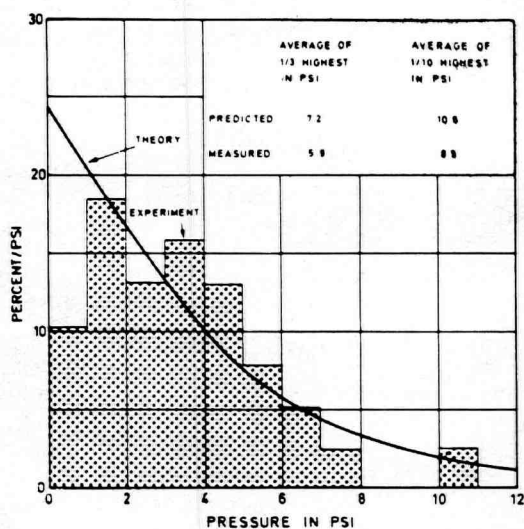
I. Strength of Decks Exposed to Green Water

In [14], Ochi states that the deck pressure caused by "green sea" can be estimated by taking the static pressure of the difference between the relative motion (motion of the ship relative to the wave) and the freeboard (see Fig. 56).

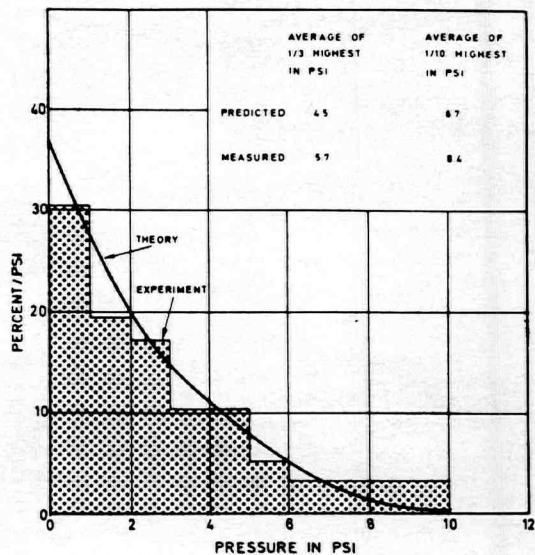
When the total amount of damage on ships in service was compared with (a) the design practice set forth by the rule requirements of our Society, and (b) the long term distribution of relative motions (previously described), a quite good agreement with Ochi's conclusions was obtained.

The full-scale observations described in [23] shows a similar trend, though this statistical material on "green sea"-pressure is not extensive enough to allow any definite conclusions.

In Fig. 57 are shown some results from a calculation on deck beams satisfying the rule requirements. The beams are T-beams. No membrane effects are included, and no



HISTOGRAM OF PRESSURE EXPERIENCED ON THE DECK DUE TO GREEN WATER (MARINER, MODERATE SEA STATE 7, SHIP SPEED 10 KNOTS, FULL DRAFT)



HISTOGRAM OF PRESSURE EXPERIENCED ON THE DECK DUE TO GREEN WATER (HIGH SPEED RESEARCH SHIP, SEA STATE 6, SHIP SPEED 20 KNOTS, DESIGN DRAFT)

Fig. 56 Comparison between theory and experiment regarding water pressures on deck. From [25]

stability considerations are made. The three pressure heights shown are the ones required to cause: (a) initial yield at the built-in ends, (b) initial yield at the center, and (c) 99 percent developed plastic hinge at the center.

The permanent deflections for the two latter loads are $l/2750$ and $l/270$, respectively.

According to the figure, the deck beams at forecastle deck are more highly stressed than those farther aft. There is a similar trend for other scantlings. The damage statistics confirm this. The majority of damages that are caused by deck pressure occur forward of $0.1L$ from FP .

Just behind the forecastle deck, the gap between the pressure height estimated from the relative motions and the design pressure height is largest. Few damages are, however, reported from this region. This may be explained by the "shading effect" of the forecastle.

Our new rules for pillars under exposed decks have been derived from our calculations of relative motions.

Acknowledgment

The work described in this paper has been carried out by the staff of the Research Department of Det norske Veritas over the past two or three years. The author wishes to record his appreciation to the many individuals who assisted in carrying out theoretical and experimental investigations, data reduction and computer analysis, drawing of graphs, and typing.

Special recognition is directed to Mr. N. Nordenstrøm and his group who have carried the burden of the work on sea loads, and to Dr. H. E. Q. Røren and his assistants who have carried out most of the work on structural response.

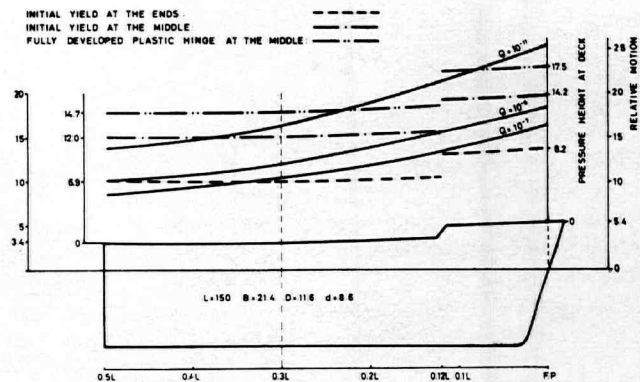


Fig. 57 Calculated deck pressures compared to pressures required to cause different types of conditions in a deck beam

References

- 1 W. J. Pierson, Jr., and L. Moskowitz, "A Proposed Spectral Form for Fully Developed Wind Seas Based on the Similarity Theory of S. A. Kitaigorodskii," *J. Geophys. Res.*, vol. 69, no. 24, 1964, pp. 5181-5190.
- 2 D. E. Cartwright, "A Comparison of Instrumental and Visually Estimated Wave Heights and Periods Recorded on Ocean Weather Ships," I.S.S.C., Delft, 1964. Comm. No. 1: Environmental Conditions. Communications to the Members.
- 3 Y. Yamanouchi, S. Unoki, and T. Kanda, "On the Winds and Waves on the Northern North Pacific Ocean and South Adjacent Seas of Japan as the Environmental Condition for the Ships," Ship Research Institute, Japan, Paper No. 5, 1965.
- 4 H. U. Roll, "Height Length and Steepness of Sea Waves in the North-Atlantic and Dimensions of Sea Waves

as Function of Wind Force," *SNAME Tech. & Res. Bull.* No. 1-19, 1958.

5 B. V. Korvin-Kroukowsky, and W. R. Jacobs, "Pitching and Heaving Motions of a Ship in Regular Waves," *TRANS. SNAME*, vol. 65, 1957, pp. 590-632.

6 W. R. Jacobs, J. Dalzell, and P. Jalongas, "Guide to Computational Procedure for Analytical Evaluation of Ship Bending Moments in Regular Waves," Davidson Lab. Rep. No. 791, 1960.

7 O. Grim, "Die Schwingungen von Schwimmenden Zweidimensionalen Körpern," *Hamb. Schiffbau-Versuchsanst. Bericht Nr. 1171*, 1959.

8 J. Fukuda, "Computer Program Results for Response Operators of Ship Motions and Vertical Wave Bending Moments in Regular Waves," Kyushu University Faculty of Engineering, Feb. 1966.

9 Y. Watanabe, "On the Theory of Heave and Pitch of a Ship," Kyushu University Faculty of Engineering Technol. Rep., vol. 31, no. 1, 1958.

10 F. Tasai, "On the Damping Force and Added Mass of Ships Heaving and Pitching," Research Institute Applied Mechanics (Kyushu University) Rep., vol. VII, no. 26, 1959 and vol. VIII, no. 31, 1960.

11 G. Vossers, W. A. Swaan, and H. Rijken, "Experiments With Series 60 Models in Waves," *TRANS. SNAME*, vol. 68, 1960, pp. 364-450.

12 W. A. Swaan and G. Vossers, "The Effect of Forebody Section Shape on Ship Behaviour in Waves," *R.I.N.A. Trans.*, vol. 103, 1961, pp. 297-328.

13 E. V. Lewis and R. Bennet, "Lecture Notes on Ship Motions in Irregular Seas," Webb Institute of Naval Architects, Oct. 1963.

14 M. K. Ochi, "Extreme Behavior of a Ship in Rough Seas—Slamming and Shipping of Green Water," *TRANS. SNAME*, vol. 72, 1964, pp. 143-202.

15 D. I. Fritch, F. C. Bailey, and N. S. Wise, "Results from Full-Scale Measurements of Midship Bending Stresses on Two C4-S-B5 Dry-Cargo Ships Operating in North Atlantic Service," Ship Struct. Comm. Rep. SSC-164, 1964.

16 N. Nordenstrøm, "Further Analysis of Full-Scale Measurements of Midship Bending Moments," Chalmers University of Technology, Div. of Ship Design, Gothenburg, 1965.

17 A. J. Johnson and E. Larkin, "Stresses in Ships in Service," *R.I.N.A. Trans.*, vol. 106, 1964, pp. 1-25.

18 M. Yoshiki, et al. "Experiments on the Strength of Container Ships," Shipb. Res. Assoc., Japan. Rep. No. 40, 1964.

19 E. M. Q. Røren, "Torsion of Hulls Having Wide Hatches, Experiment and Theory," *European Shipbuilding*, vol. 16, No. 2, 1967.

20 G. de Wilde, "Structural Problems in Ships With Large Hatch Openings," *Internat. Shipb. Progr.*, vol. 14, no. 149 and 150, 1967.

21 W. K. Meyerhof, "Die Berechnung Hydroelastischer Stösse," *Schiffstechnik*, 12, no. 60 and 61, 1965.

22 H. S. Townsend, "Some Observations on the Shape of Ship Forebodies with Relation to Heavy Weather," *SNAME*, New York Metropolitan Section, April 1960.

23 Shipbuilding Research Association of Japan: "Experiments on the Stress Frequency and Deck Wave Load Acting on the High Speed Ships in Rough Seas," Shipb. Res. Assoc. Japan. Rep. No. 49, 1965.

24 D. Hoffman, "Distributions of Wave-Caused Hydrodynamic Pressures and Forces on a Ship Hull," Norwegian Ship Model Experimental Tank Publ. No. 94, 1966.

25 M. K. Ochi, "Prediction of Occurrence and Severity of Ship Slamming at Sea," Fifth Symposium of Naval Hydrodynamics, Office of Naval Research, U.S.A. and Shipsmodelltanken, Bergen, Norway, 1964.

26 J. B. Caldwell, "Ultimate Longitudinal Strength," *R.I.N.A. Trans.*, vol. 107, 1965, pp. 411-430.

27 H. A. Schade, "Thin-Walled Box Girder—Theory and Experiment," *Schiff und Hafen*, vol. 17, no. 1, 1965, pp. 2-9.

28 J. J. W. Nibbering, "An Experimental Investigation in the Field of Low-Cycle Fatigue and Brittle Fracture of Ship Structural Components," *R.I.N.A. Trans.*, vol. 108, 1966, preprint.